SKIN TISSUE WELDING WITH NEAR INFRARED LASERS: INVESTIGATION OF THE OPTIMAL PARAMETERS

by

HAŞİM ÖZGÜR TABAKOĞLU

BSc., in Molecular Biology and Genetics, Bogaziçi University, 2000

MSc., in Institute of Biomedical Engineering, Bogaziçi University, 2003

Submitted to the Institute of Biomedical Engineering

in partial fulfillment of the requirements

for the degree of

Doctor

of

Philosophy

Boğaziçi University

January 2010

SKIN TISSUE WELDING WITH NEAR INFRARED LASERS: INVESTIGATION OF THE OPTIMAL PARAMETERS

APPROVED BY:

Assoc. Prof. Murat GÜLSOY .....
(Thesis Advisor)

Assoc. Prof. Ata AKIN .....

Assoc. Prof. Burak GÜÇLÜ .....

Prof. Hale SAYBAŞILI .....

Prof. İnci ÇİLESİZ .....

DATE OF APPROVAL: 19.1.2010

ACKNOWLEDGMENTS

...To my family and to my wife Baharım.

I would like to thank my supervisor Assoc. Prof. Murat Gülsoy, for not only his encouraging guidance, but, the most important for me, for his ability at looking events from different points of view that contributes me for overcoming difficulties during the time of this study.

I would like to thank Assoc. Prof. Ata Akın and Assoc. Prof. Burak Güçlü for being a member for my thesis committee as well as my thesis progress committee and their valuable contributions and suggestions.

I want to thank Prof. Hale Saybaşılı for being a member for my thesis committee.

Our lighthouse Prof. İnci Çilesiz, thank you for your guidance and support, providing 980 nm diode laser for experiments, and for being a member for my thesis committee.

I would like to thank Prof. Reşit Canbeyli for his contributions to make this study possible in Boğaziçi University Psychobiology Laboratory.

This thesis work was supported financially by funds listed below
TÜBİTAK: Project no: 104M428 and Project No: 107E119
Boğaziçi University Research Fund Project No: BAP-06M102.

ABSTRACT

SKIN TISSUE WELDING WITH NEAR INFRARED LASERS: INVESTIGATION OF THE OPTIMAL PARAMETERS

Laser tissue welding/soldering is an alternative to conventional closure techniques in surgery. In the present study, the closure capability and the contribution to recovery period of laser welding techniques were investigated through comparative experiments. Effects of three near infrared (NIR) wavelengths, *809 nm* diode laser, *980 nm* diode laser and *1070 nm* ytterbium fiber laser, were compared not only among themselves but also with classical manual suturing for skin closure competency. Lasers with different NIR wavelengths were delivered to skin incisions via optical fibers and laser power was adjusted according to predosimetry studies. In dosimetry experiments all the three NIR lasers were tested for their efficacy in welding; besides, 809 nm diode laser was also tested for its efficacy in laser soldering. Effects of 980 nm laser welding at same energy but different irradiation levels were also compared. Throughout this period, healing was inspected at particular days (1, 4, 7, 14, 21) by histological and mechanical methods. Skin samples were stained with Hematoxylin and Eosin (H&E) in order to assess gross pathological changes along epidermis and dermis created either by photothermal laser tissue interactions or suturing and suture material itself. These changes were quantified as closure index (CI), thermally altered area (TAA), granulation area (GA) and epidermal thickness (ET) by using different microscopy techniques such as brightfield, polarized light and phase contrast. The laser welding techniques were found reliable in terms of immediate and mechanically strong closure compared to suturing.

Keywords: Skin welding/soldering, 809 nm diode laser, 980 nm diode laser, 1070-nm YFL, ICG, Tensile test, H&E staining, Closure index.

ÖZET

YAKIN KIZILALTI LASERLERLE DOKU KAYNAĞI: OPTİMAL PARAMETRELERİN ARAŞTIRILMASI

Laser doku kaynağı/lehimlemesi cerrahi uygulamalarda geleneksel kapatma yöntemlerine bir alternatif olarak sunulmaktadır. Bu çalışmada, laser doku kaynağı tekniklerinin iyileşme sürecine sağladığı faydalar ve dokuyu kapatabilme yetisi karşılaştırmalı deneylerle araştırılmıştır. Üç yakın-kızılaltı dalgaboyunda yapılan ışımanın, 809 nm diyot laser, 980 nm diyot laser, ve 1070 nm ytterbium fiber laser, deri kapatma yetileri ve etkileri hem kendi aralarında hem de klasik dikiş yöntemiyle karşılaştırılmıştır. Laser enerjisi dokuya optik fiberler yardımıyla aktarılmış ve laser güçleri ön doz-kestirim çalışmaları ile belirlenmiştir. Ön doz kestirim deneylerinde her üç dalgaboyu doku kaynağı için denemiştir, bunun yanında 809 nm diyot laser doku lehimlemesi için de test edilmiştir. Indosiyanin yeşil ve sığır serum albumin karışımı lehim maddesi olarak kullanılmıştır. Aynı enerjide, farklı güç yoğunluğu düzeylerindeki 980 nm laser kaynağı etkileri araştırılmıştır. Bu süreç içerisinde iyileşme belirli günlerde histolojik ve mekanik olarak takip edilmiştir. Laser doku etkileşiminin ışıl-ısıl özelliğinden veya dikiş tekniğinden kaynaklanan epidermal veya dermal histopatolojik değişikliklerin tespiti için deri örneklerinde Hematoksilen-Eosin boyama yöntemi kullanılmıştır. Bu değişimler farklı mikroskopi teknikleri yardımıyla (parlakalan, polarize, faz-kontrast) kapanma indeksi, ısıl değişim alanları, granülasyon alanları, ve epidermal kalınlık şeklinde sayısallaştırılmıştır. Laser kaynağı teknikleri dikiş tekniğine kıyasla mekanik olarak güçlü ve hızlı bir kapatma sağlaması açısından daha güvenilir bulunmuştur.

Anahtar Sözcükler: Deri kaynağı/lehimi, 809 nm diyot lazer, 980 nm diyot lazer, 1070 nm YFL, ICG, Çekme testi, H&E boyama, Kapanma indeksi.

TABLE OF CONTENTS

LIST OF FIGURES

LIST OF TABLES

LIST OF SYMBOLS

λ	the wavelength of lasers
δ	penetration depth of wavelength

LIST OF ABBREVIATIONS

NIR	Near Infrared
ICG	Indocyanine Green
BSA	Bovine Serum Albumin
HI	High Irradiation
LI	Low Irradiation
SMA	Sub Miniature version A
S	Suture
W	Watt
nm	Nanometer
cm	Centimeter
J	Joule
CO_2	Carbon Dioxide
Ho:YAG	Holmium:Yttrium Aluminum Garnet
Nd:YAG	Neodymium:Yttrium Aluminum Garnet
Er:YAG	Erbium:Yttrium Aluminum Garnet
He:Ne	Helium:Neon
GaAlAs	Gallium-Aluminum-Arsenide
KTP	Potassium-titanyl-phosphate
$AgCl_xBr_{1-x}$	Silver Halide Crystal
EM	Electron Microscopy
TFC	Thermal Feedback Control
CI	Closure Index
TAA	Thermally Altered Area
GA	Granulation Area
ET	Epidermal Thickness
TS	Tensile Strength
mm	Millimeter
mg	Milligram

PBS	Phosphate Buffered Saline

1. INTRODUCTION

1.1 Motivation

From endoscopic minimally invasive surgery to open heart surgery, any kind of surgical intervention requires an incision or a small hole on skin tissue that must be closed watertight in order not to let pathogens pass through inside the body after application. Not only skin tissue but also hollow organs, arteries and veins need to be anastomosed depending on the type of surgery.

Although conventional mechanical techniques are reliable that have proven themselves over the years to be good clinical practice, neither suturing nor stapling can provide leakproof closure, on the contrary new holes are created. It is difficult to apply suture in laparoscopy where optical fibers are better suited. Bioadhasive glues are also used for wound closure and can seal incision watertight, however they are cytotoxic. Besides they cannot be absorbed by tissue and cause foreign-body granulomas and allergic reactions.

Laser tissue welding is alternative to conventional mechanical closure techniques having advantages of reduced operation times, reduced skill requirements, no needle trauma, reduced foreign body reaction, reduced bleeding and may be the most important immediate watertight anastomosis. High number of injuries occur at natural disasters, traffic accidents or wars. Bleeding must be ceased urgently and mechanically strong tissue closure should be provided so that high number of people can be treated in a short period of time. In addition, immediate closure accelerates wound healing thus allowing for a quick return to normal activity.

The aim of the dissertation is to find optimal laser welding/soldering parameters on skin tissue with near infrared lasers.

1.2 Objectives

1. To find out optimum laser irradiance levels, for 809 nm, 980 nm and 1070 nm lasers, that can bond skin tissue without any thermal hazard such as carbonization.

2. To examine effect of albumin-indocyanine green soldering on welding with 809 nm diode laser.

3. To put forward how high level and low level irradiances differ in skin welding with same wavelength (980 nm)

4. To compare skin closure abilities of near infrared laser wavelengths (809 nm, 980 nm and 1070 nm) at equal irradiance level among themselves and manual suturing by quantifying histological indications and measuring mechanical strength.

5. To follow up the 21 days recovery period of the surgical skin incisions closed with either of the mentioned techniques above through particular days.

1.3 Overview

Background about the laser tissue welding/soldering and literature survey is given in next chapter.

In Chapter 3, *in vivo* operations on Wistar rat skin, information about laser systems (809 nm diode, 980 nm diode and 1070 nm fiber) and laser delivery conditions, suturing, histology (tissue processing, paraffin embedding, tissue sectioning, Hematoxylin and Eosin staining), tissue closure parameters (closure index, thermally altered area, granulation tissue area and epidermal thickness) and the way they are quantified and tissue mechanical (tensile) testing are explained

In Chapter 4, low level irradiance dosimetry studies for each laser system with brief description of experimental design, comparative studies of high and low level ir-

radiances of 980 nm diode laser and of NIR lasers among each other are explained. Result are discussed in macroscopic and microscopic scales accordingly. Closure histology parameters and closure strength are compared throughout 21 days healing period in order to determine success of the applications.

In Chapter 5, overall study is evaluated such that accomplishments of this study could be turned into a product that will be used in clinic.

2. BACKGROUND OF LASER TISSUE WELDING AND SOLDERING

Biomedical research groups are searching for improved wound healing. Sealing a cut with beam of light to its immaculate state like in science fiction movies seems far to be accomplished that is like earlier men's desire to fly. Will humanity eventually be able to come closer the supernatural healing? The efficacy of wound closure strategies will need to be tested step by step in scientific manner.

Closure or anastomosis of tissue by laser welding and soldering occur due to two phenomena: First one is physical that is thermal and optical interactions of laser with tissue and the second one is biological that is modifications of connective tissue proteins during heating process and reassembly. Since the first application in 1964 on small blood vessels with Nd:YAG laser by [1], different laser systems have been at different tissue types, have transferred from laboratory testing to approved clinical practice [2]. The first attempt came from Schober *et al* [3] about finding molecular level changes of laser irradiated tissue (Figure 2.1) but process that is change in collagen fiber bundles with interdigitation of altered individual tropocollagen units, denaturation and cross-linking of tissue proteins appeared to be structural basis of the welding effect, could not be understood thoroughly [4-11].

Tissue repair itself naturally is thought to occur in three phases and followed by various histological staining techniques: (I) cellular migration and inflammation for several days; (II) proliferation of fibroblasts for 2 to 4 weeks, with new collagen synthesis; and (III) remodeling of the scar from 1 month to 1 year, a process that includes collagen cross-linking and active collagen turnover [12], in general. Healing phase further divided into phases of coagulation, inflammation, matrix synthesis and deposition, angiogenesis, fibroplasia, epithelialization, contraction, and remodeling, [13-15] in detail. Fibroblast cells, as being the principal source of collagen and wound connective tissue, begin to synthesize and secrete measurable amounts of extracellular collagen

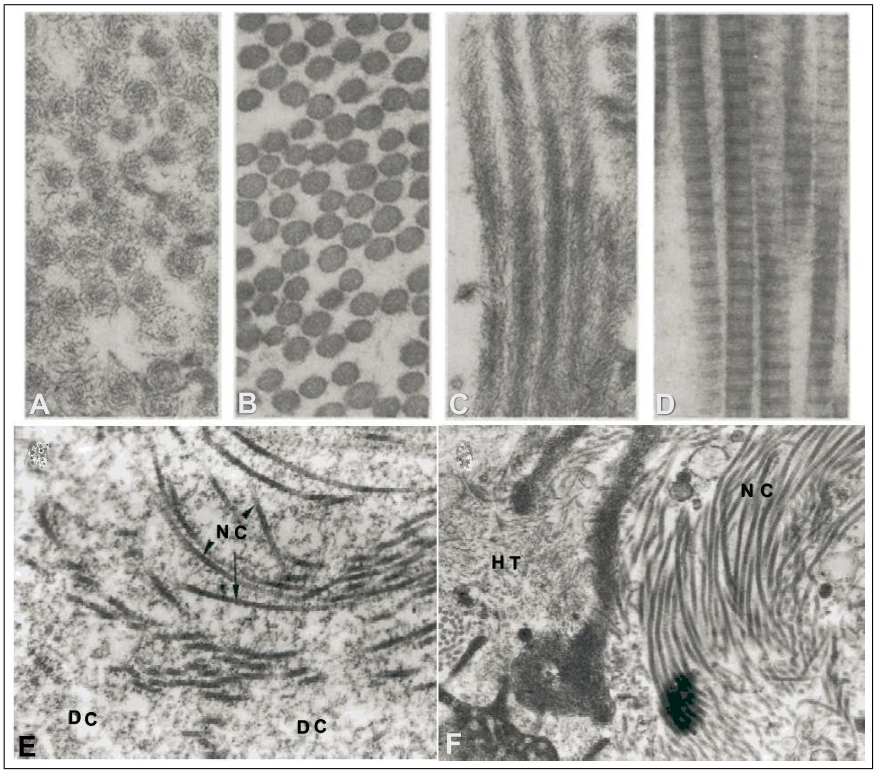

Figure 2.1 Ultrastructure of laser-induced adventitial collagen alteration in cross (A) and longitudinal (C) section. The welding effect becomes apparent by comparison with nonirradiated areas at the same magnification (B and D), x32,000 (E) Dissolved collagen fibers DC, interspersed between normal collagen fibers NC presenting clear periodicity. EM; x30,000. (F) high density of newly formed collagen fibers NC neighboring homogenized tissue HT and located at the junction between media and adventitia. EM; x30,000 [3,4].

on the second or third day after wounding. Polymerization of collagen fibers occurs in extracellular wound environment where monomers of collagen are secreted. Tensile strength of collagen fibers increases as increase in covalent cross-linking among fibers. At 1 week following wounding, immature collagen fibers become histologically apparent in the wound [13, 16-18].

Requirement of mechanical assembly in any skin cuts or surgical incisions was carried out by using conventional mechanical closure techniques for tissue bonding (sutures, staples, and adhesives) are highly reliable procedures that have proven themselves over the years to be good clinical practice [19-25]. These methods are favored due to reliability, cost-effectiveness and suitability of any type of tissue. The primary function of the suture is to maintain tissue approximation during healing. Sutures placed in the dermal layer provide tensile strength, and control tension for the outer

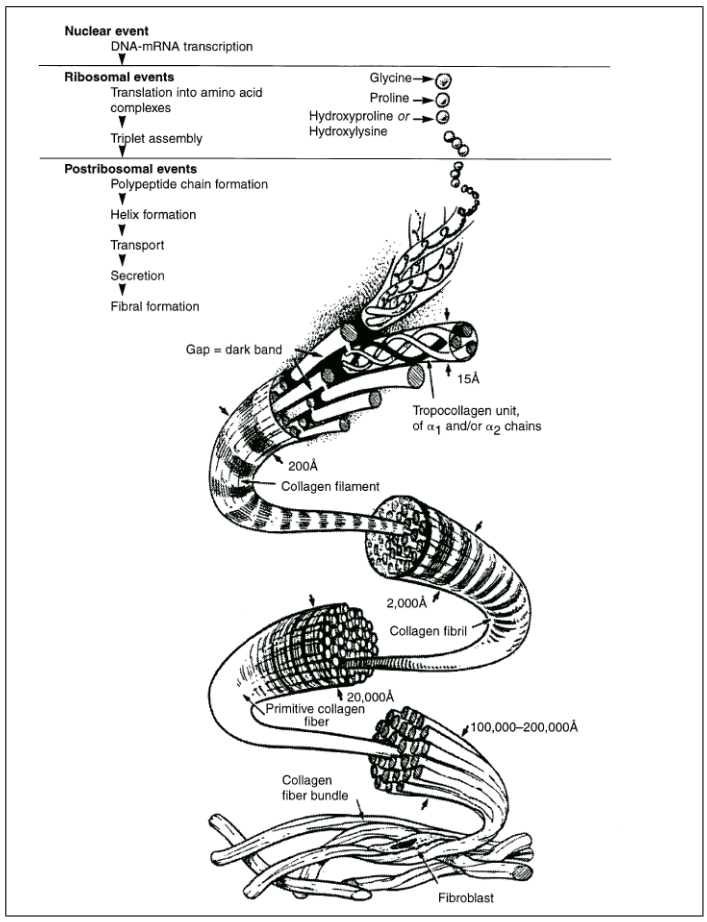

Figure 2.2 Molecular and fibrillar structure of collagen [13].

layer [19, 26, 27]. In the selection of a suture, a patient health status, age, weight, and the presence or absence of infection are as important as the biomechanical properties of the suture, individual wound characteristics, anatomic location, and a surgeon's personal preference and experience in handling a suture material. Fundamental intention to any surgeon is choosing a method of closure that affords a technically easy and efficient procedure, secure closure, minimal pain and scaring. However, these conventional fasteners cause tissue injury due to their mechanical penetration. Foreign body reaction is given rise because of nature of materials used [28, 29]. Tissue injury and foreign-body reaction can induce inflammation, granuloma formation, scarring, and stenosis [30]. Sutures may not be suitable for microsurgical or minimally invasive endoscopic applications [31]. Precision of alignment is so hard for staples and clips due to relatively large force requirements for positioning. Most importantly, none of these fasteners produces a watertight seal over the repair [32]. Besides the mechani-

cal closure methods, FDA approved biological and non-biological topical skin adhesive chemicals such as fibrin glue and cyanoacrylate based compounds have been used in skin edges of wounds from surgical incisions, and simple, trauma-induced lacerations [24, 33-35]. Adhesives may be used in conjunction with, but not in place of, deep dermal stitches. Chemical bonding of tissue has contraindications over hypersensitive patients to cyanoacrylate or formaldehyde, wound with evidence of infection, mucosal surfaces [36, 37]. They are toxic to the tissues, not absorbed in the normal wound healing process, and cause foreign-body granulomas and allergic reactions.

Increased immediate wound strength, fluid-tight closure, reduced probability of infection are the advantages of laser tissue closure over conventional mechanical methods [32, 38-41]. On the other hand, thermal damage to tissue was the biggest handicap of this technique. This is an unwanted event opposed to the objective of laser tissue repair methods that is to obtain coagulation of a desired volume of tissue with minimal effects in the surrounding tissue. Endpoint decision for the tissue apposition and poor reproducibility are the other negative sides of application [42]. Optimization of laser tissue closure is quite hard due to high number of tissue optical and thermal parameters as well as laser parameters. Tissue optical and thermal parameters cannot be changed but by addition of any external agent laser light can be localized in a specific tissue region. On the other hand, laser parameters such as wavelength, fluence or irradiance, pulse duration, repetition rate, irradiation time and spot size can be adjusted to get successful tissue closure [2, 42, 43]. In the following sections optimization studies of any of these parameters will be introduced.

Tissue Closure and Anastomosis by Medical Lasers

Laser tissue closure is a non-contact method aiming to bond biological tissue with the laser energy. Mainly two types of tissue welding can be defined: Laser Welding and Laser Soldering. In order to produce bonding, target tissue is heated up with laser application in laser welding method. In the second type of application, use of soldering materials and wavelength specific absorptive dyes can enhance tissue sealing with the selective heating of target tissue.

Photothermal interaction occurs in a way that, laser (photon) energy, applied directly to the tissue surface is converted to the heat energy by molecular vibration of tissue chromophores such as water, melanin, hemoglobin by absorption (Figure 2.3). The rate of heat generation depends on the rate of absorption of photons within the tissue [44]. Scattered light that is absorbed may cause heating outside the laser beam. Increase in temperature to a certain degrees causes structural changes (interdigitation) in tissue proteins such as collagen and fibrinogen, in a way that they can bond each other in their open sites at the cooling phase. Overheating of tissue can cause immediate irreversible damage of the structural proteins of the tissue (Table 2.1). Thermal response of laser irradiated tissue have been examined in detail and modeled by Welch *et al* [44-48].

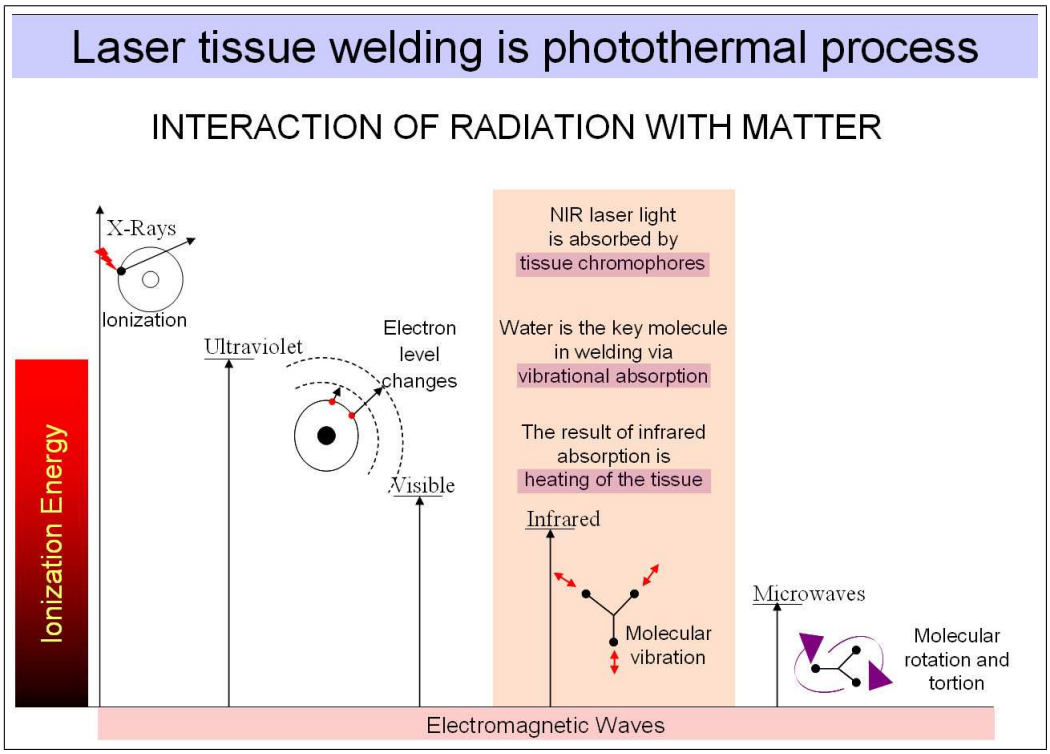

Figure 2.3 Heating of tissue by infrared mediated molecular vibration.

Wide range of medical lasers has been used for laser tissue welding. Lasers mainly operate in infrared region such as carbon dioxide (CO_2), thulium-holmium-chromium, holmium, thulium, and neodymium rare-earth doped garnets (THC:YAG, Ho:YAG, Tm:YAG, and Nd:YAG, respectively), and gallium aluminum arsenide diode (GaAlAs) lasers are suitable for tissue welding [49-52]. The CO_2 laser has been favored

Table 2.1
Laser Tissue Interactions: Photothermal Effects [44].

Temperature	Molecular and Tissue Reactions
42-45 ^{o}C	Hyperthermia leading to protein structural changes hydrogen bond breaking, retraction
45-50 ^{o}C	Enzyme inactivation changes in membrane permeabilization, oedema
50-60 ^{o}C	Coagulation, protein denaturation
$\sim$ 80 ^{o}C	Collagen denaturation
80-100 ^{o}C	Dehydration
$>$100 ^{o}C	Boiling, steaming
100-300 ^{o}C	Vaporization, tissue ablation
$>$300 ^{o}C	Carbonization

for laser repair of thin tissues due to its short penetration depth shorter than 20 μm) in tissue (Table 2.2). On the other hand, in thick tissues, high irradiances or long exposure times are necessary for sealing of target tissue [44]. Those type of applications causes undesired consequences such as carbonization of tissue and the conduction of heat from the initial absorption zone to surrounding tissue [42].

Temperature controlled laser systems have been developed to get rid of overheating consequently thermal injury to the surrounding tissue. Researchers applied radiometric methods to determine the temperature of the surface of the heated cut and used computer assisted temperature feedback control to maintain tissue surface temperature at some desired level. The Applied Physics group at the Tel Aviv University developed a laser fiberoptic system for monitoring and controlling the temperature of a spot on the tissue surface [56, 57] for CO_2 laser welding and/or soldering. Optical fibers made of polycrystalline silver halides ($AgCl_xBr_{1-x}$), which are highly transparent in the mid-infrared spectral region (3 to 30 μm) transmits emitting infrared radiation from surface of laser application spot to radiometric detector which is connected to the personal computer. The personal computer controls the power emitted by the laser,

Table 2.2
Penetration depths of some medical lasers in water and in tissue.

Laser	λ (nm)	δ_{water} [53, 54]	δ_{tissue} [54, 55]
Argon ion	488	23 m	0.8 mm
KTP/Nd:YAG	532	16 m	1.1 mm
HeNe	632.8	4.8 m	3.5 mm
GaAlAs	780	60 cm	7 mm
	820	46 cm	8 mm
	870	25 cm	7 mm
Nd:YAG	1064	4 cm	4 mm
Nd:YAP	1080	5 cm	4 mm
Ho:YAG	2100	0.2 mm	1 mm
Er:YAG	2940	1 μm	$<$1 μm
CO_2	10600	10 μm	20 μm

and thus controls the temperature of the heated spot. The system has been tried in various kinds of tissues. Skin tissue closure in rabbits, wound healing pattern was observed on 3^rd, 7^th, 14^th and 28^th post operative days of healing period by Simhon et al. [58]. Laser application along incision was done spot by spot. The mean laser power density at the heated spots was 7 W/cm^2. The spot size was 3 mm in diameter on tissue surface. Signs of thermal injury were evaluated, by signs of basophilic coloring, necrosis or carbonization residues, the presence of surface albumin residues as compared to glued or sutured scars, the degree of re-epithelialization, histologically. Laser skin closure with thermal control was found to be more successful to other wound-closure modes. Thermal damage was minimized by the use of a temperature controlled fiber optic laser-soldering system. Tensile test performed as a complimentary for this study [59] revealed immediate tensile strength values that were comparable to those obtained with cyanoacrylate glues. Moreover, laser-soldered incisions exhibited stronger long-term tensile strength and presented better wound healing behavior, compared with sutured incisions.

In vivo study was also performed in porcine model by Simhon *et al.* [60] aiming toward clinical trials by evaluating the efficacy, reproducibility, and safety of the temperature controlled laser system procedure in juvenile and mature domestic farm pigs. 500 mW CO_2 laser power was applied to the skin tissue. It was found that application at temperatures below 60°C resulted in a high dehiscence rate during trimming of the skin samples, whereas at temperatures exceeding 70°C, excessive thermal damage occurred. Therefore, the optimal soldering temperature has to be within the range of 65°C to 70°C. At this range of soldering temperatures, it is possible to immediately achieve adequate tensile strength and tight sealing of the wound, features that are difficult to achieve by the standard gluing or suturing procedures.

The system has been tried also in soft tissue (urinary bladder) welding in different animal models: Rats, rabbits, and cats. It was found that 24 hours after welding, there was a continuous muscular layer with small amount of fibrin and hemorrhage and interruption of this layer only at the site of incision. Ten days and thirty days after welding, the bladder wall looked normal with no sign of interruption, inflammation, or scar. Studies of the control group (closure with standard suture) showed that after 24 hours there was interruption of the entire bladder wall, with an acute inflammatory reaction. Ten days after closure, normal epithelial layer appeared but with interruption of the muscular layer with acute inflammation and foreign body reaction near the sutures [61].

Rat intestine argon laser (operates at multiple visible wavelengths from 488 nm to 515 nm, irradiance was 28 W/cm^2) tissue fusion was carried out by Çilesiz *et al.* [62] found that laser-assisted intestinal anastomoses provided an immediate fluid-tight seal compared to the suture control anastomoses. Less thermal damage and carbonization were seen when laser irradiation was controlled by thermal feedback. At 3 weeks, all anastomoses were mechanically as strong as intact intestine, although bursting/leaking pressure tests of laser-assisted anastomoses without thermal feedback control (TFC) tended to be lower than all sutured anastomoses (control) group and laser tissue welding with TFC group. Experimental findings indicated that; although welds were initially weak, they were sufficiently stabilized to resist spontaneous rupture

in surviving animals. In similar study performed by Çilesiz *et al.*, Ho:YAG (2.09 μm, irradiance was 16 W/cm^2) laser was used to anastomose rat intestine with and without TFC at 90°C [63]. Comparisons of the argon and Ho:YAG laser-assisted bonds with and without TFC and the suture controls showed similar wound healing patterns, tissue composition, and progression with some exceptions. The findings indicated that TFC stabilized laser assisted rat intestinal welds in vivo in the 24-72 hour postoperative period, by a decreased incidence of postoperative complications. Comparisons of two different lasers showed no differences, and variations could be attributed to nonspecific abscess formation and surgical technique. Çilesiz concluded that TFC does not provide a satisfactory method to identify the completion of a clinically successful weld. Using TFC to control rate of tissue coagulation, future studies should be done to identify end points that mark bond stability and strength.

Simple and easy-to-apply methods are demanded in minimally invasive surgery. In a study performed by Spector *et al.* [64] small bowel harvested from 6-month-old pigs was successfully anastomosed by using albumin stent heated up by a 828 nm GaAs semiconductor laser diode which emission was delivered to the tissue by 600 μm silica fiber. Both the laser delivery fiber and the radiometer fiber was designed to be positioned 8 mm from the tissue, producing a 3.4 mm diameter spot with a maximal power density of 30 W/cm^2. Albumin stent laser anastomosis of bowel sustained statistically significant higher bursting pressures than those done by sutures.

The addition of solder materials (blood, fibrinogen, albumin) and wavelength-specific chromophore help to strengthen the wound, to maintain edge alignment and to focus energy to the target region. Furthermore, due to the increased absorption characteristics of the dyed tissue or solder, low-level laser powers may be used to achieve the required effect, increasing the safety of the technique. The combination of serum albumin and ICG dye with an 800 nm diode laser, has been tried in numerous of applications in order to find optimal solder composition [64-70]

One of the most comprehensive study was performed by McNally *et al* [71] to investigate the relative importance of these parameters to laser tissue soldering. Twenty-

five different combinations of laser irradiance (6.4, 12.7, 19.1, 25.5, 31.8 W/cm^2) and exposure time (20, 30, 40, 50, 100 or 40, 60, 80, 100, 200 seconds) were used. The effect of changing bovine serum albumin (BSA) concentration (25% and 60%) and indocyanine green (ICG) dye concentration (2.5 mg/ml and 0.25 mg/ml) of the protein solder on the tensile strength of the resulting bonds was investigated on *ex vivo* aorta specimens irradiated with 808 nm diode laser delivered 400 μm-core silica fiber. Spot size at the protein solder surface was 1 mm. The effect of hydration on bond stability was also investigated using both tensile strength and scanning electron microscopy analysis. It was observed that the liquid and solid protein solders exhibited two different mechanisms of failure. The liquid protein solder broke into two halves, but each remained attached to the tissue. The solid protein solder, however, remained intact but detached from the tissue. The overall tensile strength of repairs formed using the solid protein solder were significantly higher than the strength of the liquid protein solder repairs. The lower dye concentration of 0.25 mg/ml ICG gave better results for both liquid and solid solders. Irradiance and exposure time for optimal strength were determined from these results to be 12.7 W/cm^2 for 100 seconds with the liquid protein solder repairs and 6.4 W/cm^2 for 50 seconds with the solid protein solder repairs. The results of this investigation suggest that the strongest repairs are produced with lower irradiances of around 6.4 W/cm^2 after approximately 50 seconds exposure time by using a solid protein solder composed of 60% BSA and 0.25 mg/ml ICG.

There are still several problems associated with the technique that need to be overcome. Three disadvantages of the solid protein solder have been identified [72]. First, whether water or an absorbing dye is used as the chromophore, more energy is generally absorbed near the upper portion of the solder, closer to the laser source. Irradiation of the solder produces a temperature gradient over the depth of the solder. Depending on the temperature gradient and the laser exposure, the upper portion of the solder can become over coagulated while the solder/tissue interface remains uncoagulated. Nonuniform denaturation across the solder thickness can result in the formation of an unstable solder tissue bond. Second, the protein solder is soluble in physiological solutions before laser irradiation. In addition, as these solders are often subjected to blood dilution during operation, the solder may undergo mechanical

alteration that can weaken the solder-tissue repair. Third, the solid protein solder is very brittle and inflexible thus, not easily adapted to different tissue geometries.

Specially designed artificial solder-doped polymer membranes was tried for laser assisted tissue repair by McNally *et al.* and Hodges *et al.* [66, 72]. Both the albumin protein solder and the polymer membranes are biodegradable. This brings about the minimal foreign body reaction and infection. Porous synthetic polymer membranes were prepared from PLGA with lactic:glycolic acid ratios and poly(ethylene glycol) (PEG) with PLGA/PEG blend ratios. Average irradiances of 5.7, 11.3, and 17.0 W/cm^2 delivered to the solder surface [72]. Results showed that the solder-doped polymer membranes improved repair strength as well as flexibility during application over previous published results with albumin protein solders. In addition, slight rehydration of the solder-doped polymer membranes upon application to the tissue assists with tissue apposition.

Lauto *et al.* examined *in vitro* and *in vivo* tissue repair with laser-activated chitosan adhesive [73]. Photochemically activated chitosan gels have been shown to induce no thermal damage to tissue and to produce better sealing for air leaks than fibrin [74]. The flexibility of the chitosan adhesive permitted the ready manipulation of tissue without fear of breaking or tearing. The adhesive did not fold or breakdown when manipulated with forceps and appeared to be well suited for tissue repair. The application of the adhesive on tissue was also facilitated by its adhesiveness prior to laser activation and hydrophilic properties. A review paper about different tissue reconstruction strategies employing adhesive biomaterials currently used in surgical and experimental procedures was written by Lauto PhD. concluded that each of these adhesives has an optimal clinical application depending on its physical-chemical characteristics (adhesiveness, fluid or solid consistency, chemical or light activation for example). It is thus very likely that different bioglues will be adopted by surgeons for their specific operative procedures, instead of a single product [75].

3. MATERIALS AND METHODS

3.1 Surgical Applications

3.1.1 Animals

The experiments were conducted under a protocol approved by the Institutional Animal Research and Care Ethic Committee at Boğaziçi University (BUHAYDEK, Date:1/12/2005, No:2005-6). Male Wistar Rats, randomly selected, 7-9 months old, weighing 290-320 g, from Psychobiology Laboratory of Boğaziçi University were used in all experiments mentioned in this thesis. Rats were housed in plastic cages and maintained on a 12-h-light/12-h-dark cycle in a temperature-controlled vivarium (22±2°C). Food and water were available *ad libitum*.

3.1.2 Surgery

Wistar rats were anesthetized with ketamine (10% ketamidor, RichterPharma, AG, Wels, Austria) by intraperitoneal injection (1.65 ml/kg). Hair at the site of application was shaved. Antiseptic Poviiodex Scrub (Kim-Pa İlaç Lab. Inc. Hadımköy) was applied topically to prevent infection and desiccation of the wounds. Three pairs of 1-cm-long full-thickness incisions (over muscular layer), bilateral and parallel to the spinal cord, were done. Incisions were implemented with sterile No.11 surgical blade (Tontarra Medizintechnik GMBH, Germany). In case of bleeding, incision site was compressed and any blood remnant was cleaned from top of skin in order to prevent probable light absorption by blood remnant on the surface of skin rather than skin tissue itself. Incision was closed with near infrared lasers (either 809 nm, 980 nm or 1070 nm) or suturing that was used as control group if included in any of experiment.

3.1.3 Post-surgery

After closure, Thiocilline (Abdi İbrahim İlaç Inc., İstanbul, Turkey) was applied on each incision to inhibit any kind of microbial reactions on incisions. The length and the thickness of the incisions were checked via digital caliper (Mitutoyo, UK). No food or water was given 24-h post-surgery. Investigation of healing was performed through 4-day period for predosimetry studies and 21-day for comparative studies. 1^st, 4^th, 7^th, 14^th and 21^st days were selected as control days during healing period. On these particular days, skin samples closed either by NIR lasers or suture were collected for histology or tensile testing. During healing period, each rat was kept in separate cage until histology examination or tensile test on particular post operative days. At the end of the any experiment mentioned, rats were anesthetized first and then killed (cervical dislocation).

3.2 Closure Methods: Laser Systems and Suturing

3.2.1 809-nm Diode Laser System

The 809-nm Diode Laser System have been designed and improved in Boğaziçi University, Institute of Biomedical Engineering, Biophotonics Laboratory [76]. The system is a computer controlled high power 809 nm laser (10 W output power at 35 A applied current). User interface was developed in C programming language communicates with the controller unit of the diode laser system to set the operating parameters of the diode laser module [77]. Laser output fiber was coupled with 400 nm fiber via FC (Fixed Connection) connector to transfer laser energy to the target tissue part.

3.2.2 980-nm Diode Laser System

The 980-nm diode (OPC-D010-980-FCPS, Opto Power, Tuscon, AZ, USA) class IV laser was controlled by a microcontroller-based controller instrument, which was

designed and manufactured by our group at Biophotonics Laboratory at Institute of Biomedical Engineering, Boğaziçi University [78]. The laser unit can also be controlled using OPC remote control module provided with the system. Either control device attaches to the laser system via the 25-pin D-sub connector on the front panel. In general description, high power diode laser system has 10 W maximum optical output. The system provides output through a 1 meter fiber-optic cable. Laser was delivered to the target tissue with a 400 μm optical fiber (Spindler-Hoyer, Gottingen, Germany) via SubMiniature version A (SMA) connection. The parameters (power, exposure time, number of cycles, and on-off duration of pulses) of the laser were controlled with interface developed in LabView software (V 6.1).

3.2.3 1070-nm Ytterbium Fiber Laser

1070 nm single mode CW Ytterbium Fiber Laser System produces 20 Watts of optical power at a wavelength of 1070 nm (YLM-20-SC Series, IPG Laser GmbH, Germany). The parameters (power, exposure time, number of cycles, and on-off duration of pulses) of the laser were adjusted via LabView interface of an external controller (Teknofil Inc., Istanbul, Turkey). Device is equipped with red aiming beam (0.6 mW).

3.2.4 Laser Delivery

Laser closure was performed that six spots were applied by a handpiece made up of plexiglass material at a distance of 2 mm above 1 cm long incision (Figure 3.1). Each spot had a 2 mm diameter and they slightly overlapped onto each other. Five seconds cooling time interval was given between spots. Spot size (0.0314 cm^2) was checked with a detection card (VRC4, Thorlabs, NJ, USA) and power of the laser was checked with a powermeter (Newport 1918-C, CA, USA) before each application.

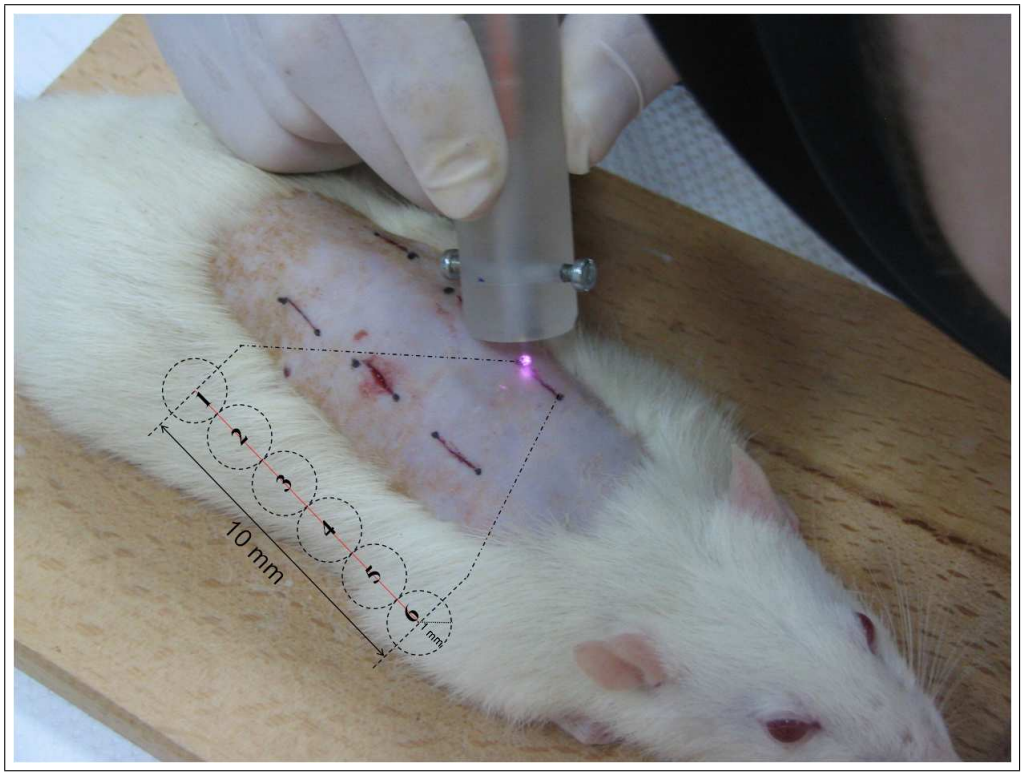

Figure 3.1 6 laser spots along 1 cm incision. 2 mm spot size was obtained from optic fiber that was placed 2 mm above skin surface.

3.2.5 Laser Safety

Laser goggles filtering either 809 nm (LG1, Thorlabs, USA), 980-nm (LG1, Thorlabs, USA), and 1070 nm (Glandale LS606, USA) were used in experiments for eye safety.

3.2.6 Suturing

A single, interrupted suture USP-3/0 metric silk (Doğsan Tıbbi Malzeme San. A. Ş. Trabzon-Turkey) was placed in the middle of the 1 cm long incisions. Distance between needle entrances to the tissue was about 10 mm.

3.3 Histology Examinations

3.3.1 Tissue Processing

Incision sites were removed one by one, in rectangular shape (1 x 2 cm) from rat's dorsal skin and stored in tissue fixative (10% PBS formaldehyde) until tissue processing. Tissue processing is dehydration of tissues in order to replace with a medium that solidifies to allow thin sections to be cut. Paraffin wax is most frequently used solidifying agent. Since it is immiscible with water, the main constituent of biological tissue, water must first be removed in the process of dehydration. Samples are transferred through baths of progressively more concentrated ethanol to remove the water, followed by a clearing agent, usually xylene, to remove the alcohol, and finally molten paraffin wax, the infiltration agent, which replaces the xylene.

Tissue processing was automatically performed by tissue processing machine (Leica TP-1020, Germany) placed in Biophotonics Laboratory, Institute of Biomedical Engineering, Boğaziçi University. Tissue samples were bathed in order of following solutions for determined time intervals (Table 3.1):

3.3.2 Paraffin Embedding

During this process the tissue samples are placed into moulds along with liquid embedding material (such as agar, gelatine or wax) which is then hardened. This is achieved by cooling in the case of paraffin wax. Formalin-fixed, paraffin-embedded tissues may be stored for a long time at room temperature, and nucleic acids (both DNA and RNA) may be recovered from them decades after fixation. Paraffin embedding was performed with heated paraffin embedding module (Leica EG1150H, Germany). Cold plate for modular tissue embedding system (Leica EG1150C, Germany) was held at a constant temperature of -5^{o}C to support rapid cooling of embedded blocks and molds. At this stage, tissue placement in casette is very crucial. Orientation was given such that frontal tissue sections can be taken, so any structural change throughout epidermis

Table 3.1
Tissue dehydration procedure.

Dehydration Procedure		
ALCOHOL	70%	1-h
ALCOHOL	70%	1-h
ALCOHOL	80%	1-h
ALCOHOL	80%	1-h
ALCOHOL	90%	1-h
ALCOHOL	90%	1-h
ALCOHOL	100%	1-h
ALCOHOL	100%	1-h
XYLENE		1-h
XYLENE		1-h
PARAFFIN	60^oC	1.5-h
PARAFFIN	60^oC	1.5-h

to muscular layer can be detected by staining (Figure 3.2).

3.3.3 Tissue Sectioning

Fully automated rotary microtome (Leica RM2255, Germany) was used for taking 5 to 10 μm thick tissue sections (Figure 3.2). These sections stretched in 40^oC water bath were placed on glass slides and put into incubator overnight in order to get rid of remaining paraffin.

3.3.4 Tissue Staining

Staining is employed to give both contrast to the tissue as well as highlighting particular features of interest. Hematoxylin and Eosin (H&E) staining was used for

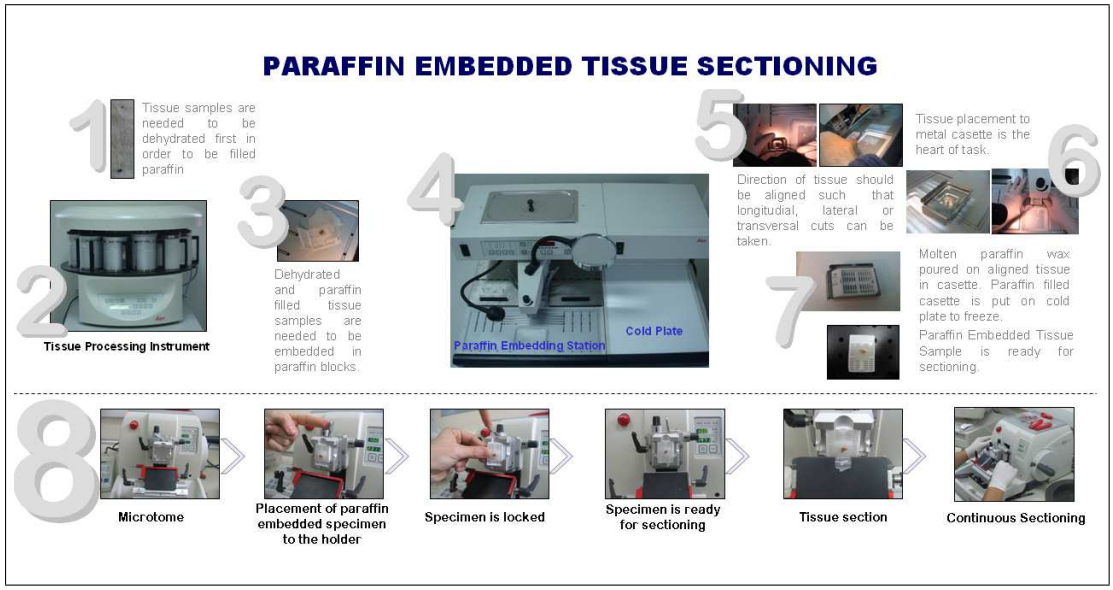

Figure 3.2 Paraffin Embedded Tissue Sectioning Method.

histological examinations. This stain gives idea about general tissue structure. Hematoxylin, a basic dye, stains nuclei blue due to an affinity to nucleic acids in the cell nucleus; eosin, an acidic dye, stains the cytoplasm, reticular and elastic fibers pink. Staining procedure is explained in Figure 3.3

3.4 Image Analysis

Histology samples were examined under light microscope (Eclipse 80i, Nikon Co., Japan) and high resolution (2560 x 1920 pixel) images were taken with 5 megapixel CCD camera (DS-Fi1, Nikon Co., Japan) either one of the techniques: brightfield light, polarized light and phase contrast condenser, to determine thermal effect of near infrared lasers to the tissue as well as tissue closure abilities. Imaging software (NIS Elements-D, Nikon Co., Japan) was used to quantify parameters which give idea on how successfully an incision closed. Mentioned parameters are: Closure Index (CI), Thermally Altered Area (TAA), Granulation Area (GA) and Epidermal Thickness (ET).

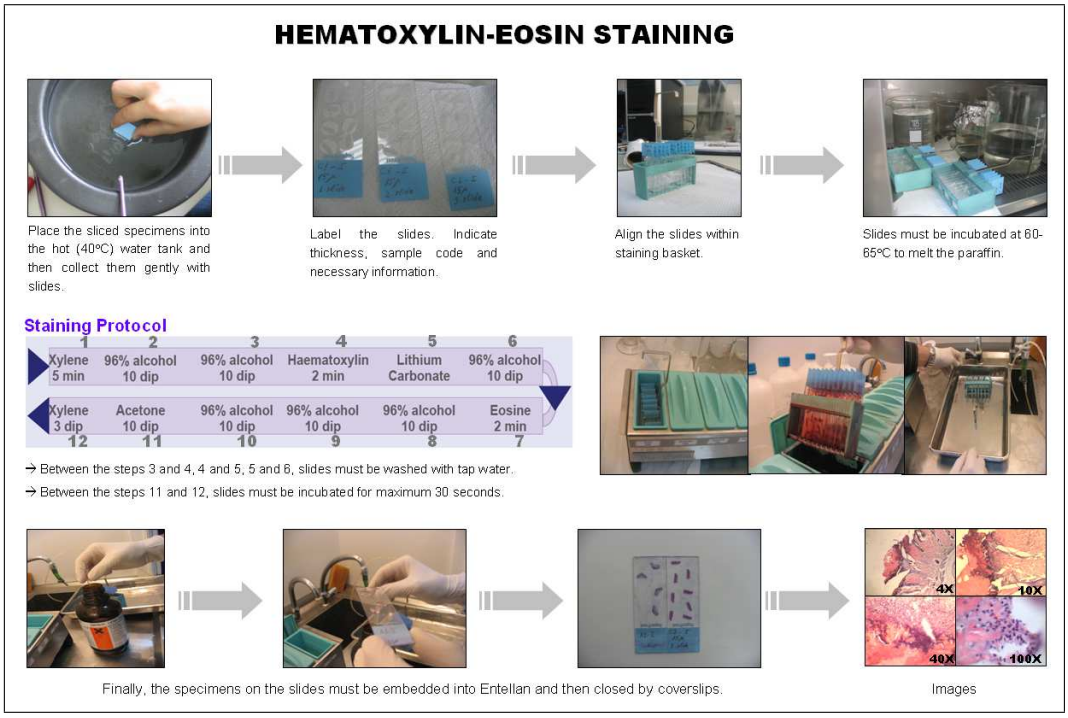

Figure 3.3 H&E stainig method.

3.5 Closure Parameters

Closure Index (CI) is the ratio of closed parts to the total incision. In order to figure out the closed parts, the summation of the non-closed segments ($\sum NC_i$) is subtracted from total incision (TI, the distance from surface of skin to muscular layer)(Figure 3.4). Subsequently CI can be calculated with the formula: CI=[TI-($\sum NC_i$)]/TI. CI values ranges from zero to one. Zero corresponds to no closure and 1 means full closure.

Thermally Altered Area (TAA) reveals information about the thermal changes of laser welded or soldered tissue part. Absorption of heat energy results in hyperthermia, coagulation, ablation, and carbonization depending on the optical and thermal characteristics of that tissue. Those changes can be identified under microscope as change in color and morphological degeneration due to denaturation of cellular structures (Figure 3.5).

Connective granulation tissue area (GA) can be observed due to the formation

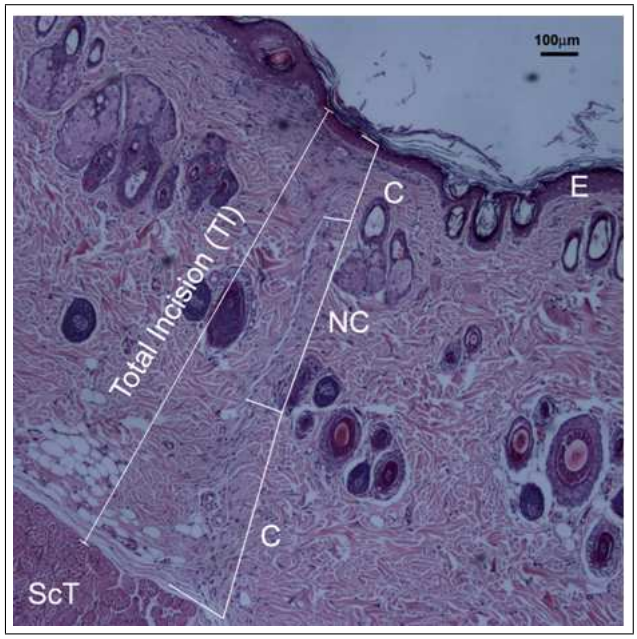

Figure 3.4 Closure Index calculation. C: Closed, NC: Non-closed, E: Epidermis, ScT: Subcutaneous tissue, TI: Total Incision. X4, H&E, Brightfield.

of new fibroblasts, inflammatory cells and capillaries during the recovery process. GA is an indicator of the overall damage given (Figure 3.6).

Epidermal Thickness (ET) of the recovered incision shows the success of welding (or suture) in terms of scar formation. Measurements of ETs were performed at 6 to 8 different points for each sample (Figure 3.7).

3.6 Tensile Test

Incision sites were removed as dumbbell-shaped stripes about 5-cm long. Tensile strength tests were performed in between 10 minutes after removal in order to minimize drying. Samples were placed between single column universal testing machine (LF Plus, Lloyd Instruments, UK) jigs' such a way that grips (TG34, Lloyd Instruments, UK) were as close as possible (2-4 mm). The machine can be used to perform tests in two modes, as a stand alone machine or under computer control with NexygenePlus software with RS232 connection. Jigs surfaces were notched like lock-and-key to prevent skin

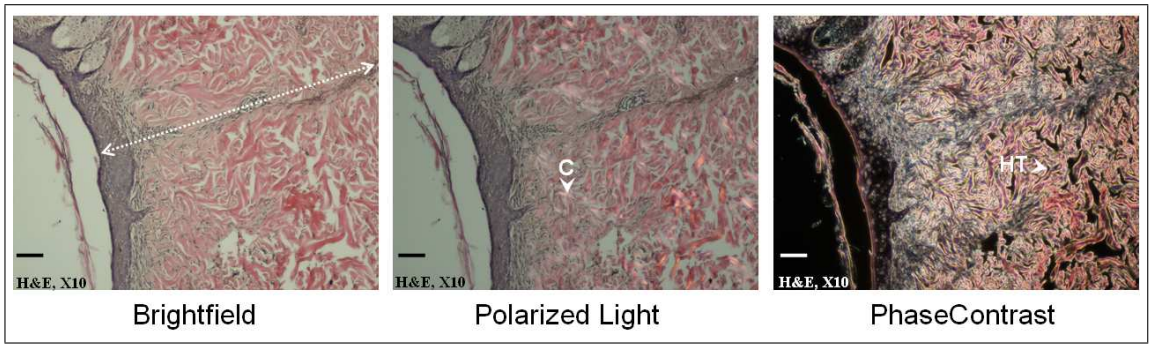

Figure 3.5 Inspection of thermaly altered areas (TAA) by using different microscopy techniques. Same image was examined with brightfield, polarized light and phase contrast microscopy. The brightfield microscopy showed overall structures of tissue sample. Incision line was shown by arrow. The polarized microscopy reveals the collagen molecules (C) that were not affected by heat. Denatured collagen molecules loose their birefringent characteristic and do not shine under polarized light. The phase contrast technique goes further and shows the hyperthermal (HT) area. H&E, X10, Scale Bar is 100μm.

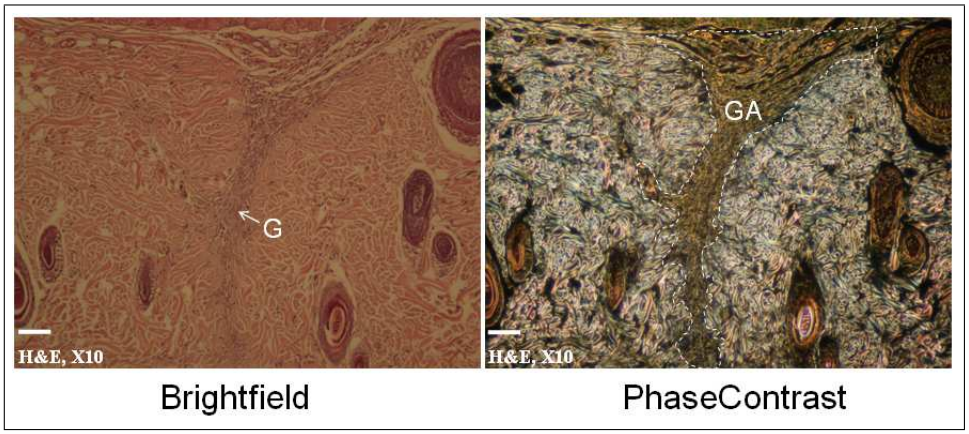

Figure 3.6 Granulation tissue is newly forming tissue after any kind of injury. The brightfield microscopy shows the granulation (G). Granulation Area (GA) was observed more clearly with the Phase Contrast technique. H&E, X10, Scale Bar is 100μm.

sample slipped through jigs (Figure 3.8). The machine is microprocessor controlled, 32 bit for load measurement. Load cell capacity was 250 N and each sample was tested at 5 mm/min crosshead velocity. Force (N) and time (s) at break point (this was determined as first opening anywhere along 1 cm long incision) were recorded by software NexygenPlus (Figure 3.8).

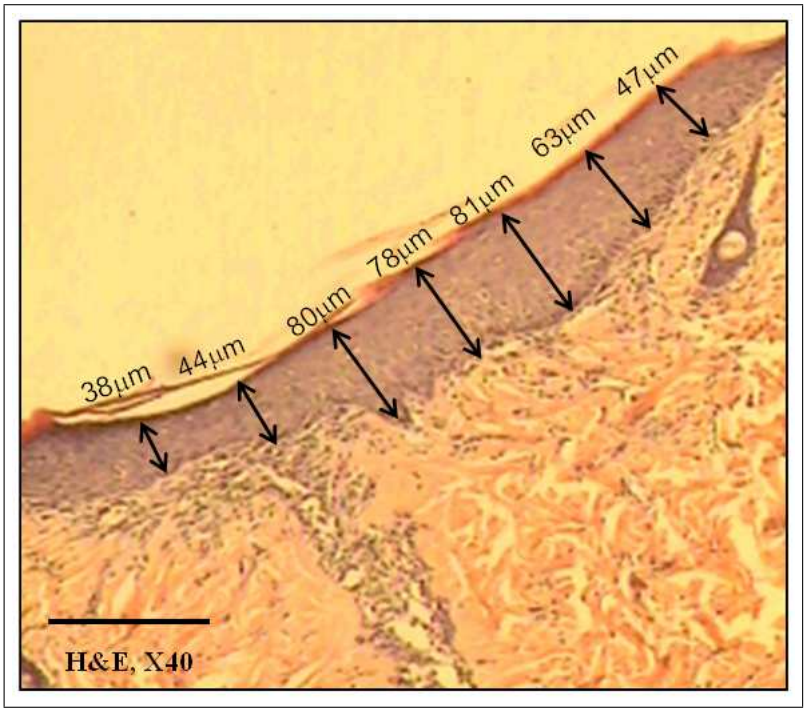

Figure 3.7 Increase in epidermis layer depends on size of the defect, the nutrient supply, and the wound environment. H&E, X40, Scale Bar is 100μm.

3.7 Statistical Analysis

Statistical analysis was performed using a two-tailed paired Student's t-test to determine statistical differences for groups as indicated. Differences with $p<0.05$ were regarded as significant.

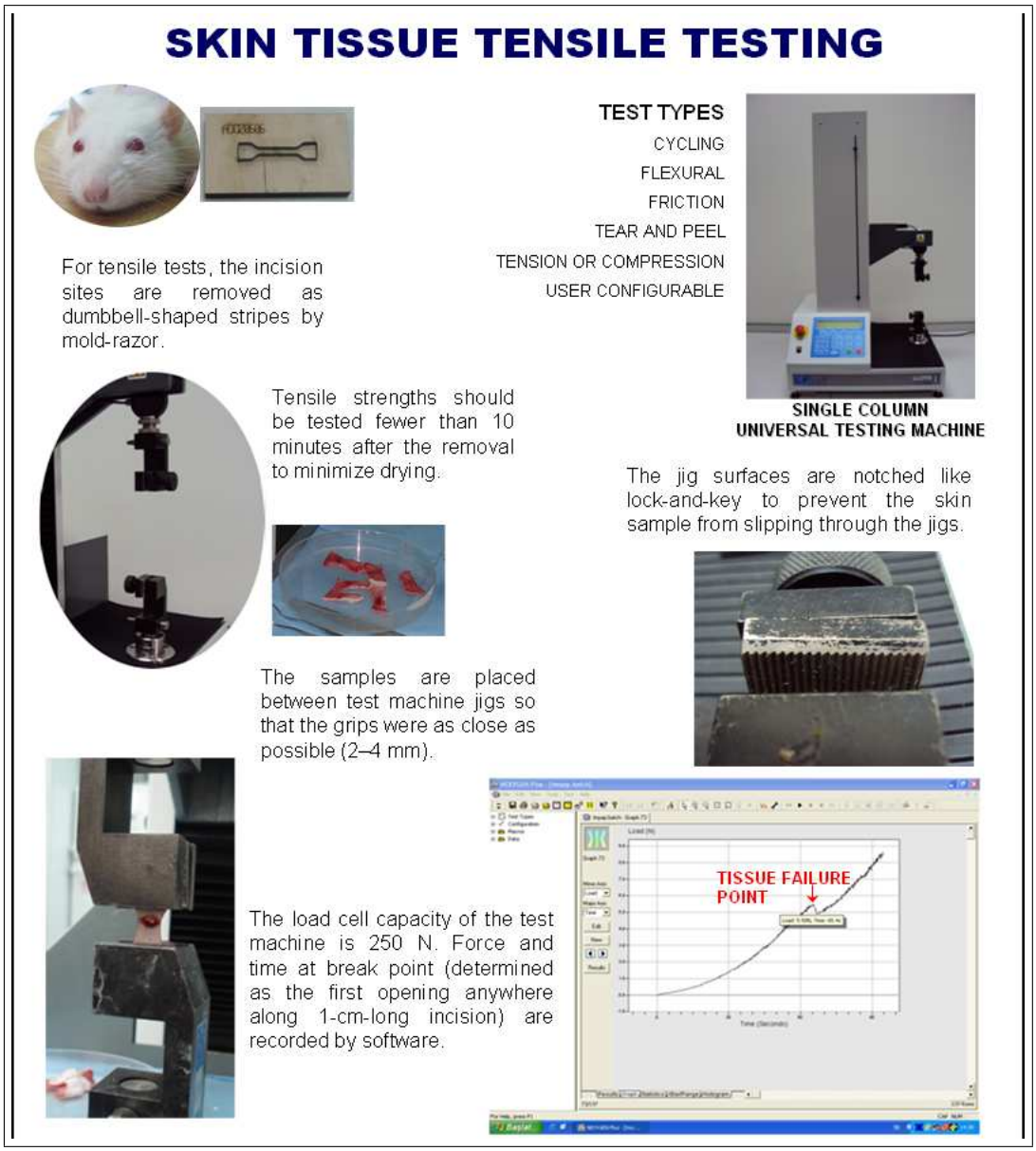

Figure 3.8 Skin Tissue Tensile Testing

4. RESULTS AND DISCUSSION

4.1 809 nm LASER TISSUE SOLDERING

This part of thesis work aims to bring out optimal 809 nm diode laser closure parameters in combination with ICG-doped bovine serum albumin solder. Laser applied with protein-based biologic or lab-made synthetic materials as solder and wavelength specific biocompatible chromophores aims to improve low adherence strength and to reduce thermal damage upon tissue. Albumin is the most preferred protein-based soldering material by researchers [79]. Bovine albumin was extracted from blood serum of bovine. Bass *et al.* was pioneering the implementation of the combination of serum albumin and indocyanine green (ICG) dye with an 800 nm diode laser [80]. The light sensitive ingredient in the protein solder is the ICG dye which has a maximum absorption coefficient at 805 nm of $2 \times 10^5 M^{-1} cm^{-1}$ [81], though collateral tissue thermal damage due to direct absorption of the laser light is minimized. Throughout the wound healing period, biocompatible solder coagulum is gradually absorbed by tissue. It is also claimed that presence of the solder coagulum increases the initial strength of the repair [32]. Withstanding applications of ICG-doped albumin protein solders have been verified in a range of studies such as peripheral nerve repair [65], colonic anastomoses [82], arteriovenous anastomoses [83], extravesical reimplantation of the ureters [84], urinary tract reconstruction [85], skin closure [86]. Determination of optimal parameters for laser skin soldering studies at 810 nm wavelength was performed by Cooper *et al.* [87] and Suh *et al.* [88] on rat skin model.

4.1.1 Solder Materials and Composition

Indocyanine Green (ICG - Pulsion Medical Systems AG, Munchen-Germany) and Bovine Serum Albumin (BSA-Fluka-BioChemika, Fraction V, Buchs - Switzerland) was used as solder materials. Ratio of solder composition was tried in a series of

trials. ICG tends to aggregate in water at high concentrations. This means that the effective absorption does not increase linearly with increasing concentration. ICG tends to degrade with exposure to light as well. The photodegradation is mitigated when ICG is bound to albumin. The photodegradation is also concentration dependent. Soldering solution was determined as composition of 25% BSA (w/v) and 2.5 mg/ml ICG dissolved in deionized water.

Bovine serum albumin (BSA)is a large globular protein (66,000 Dal) with a good essential amino acid profile. It has been well characterized and the physical properties of this protein are well known [98-90]. BSA binds free fatty acids, other lipids and flavor compounds, which can alter the heat denaturation of the protein [91]. Isolated BSA has been reported to be a very functional protein [92]. It is reported to partially unfold between 40 and 50^{o}C, exposing non-polar residues on the surface and facilitating reversible protein-protein interactions.

4.1.2 Experimental Design

6 male Wistar rats weighing 295-310 g were used. 1 cm long surgical incisions were made parallel to the spinal cord with no. 11 surgical blades (Figure 4.1). Low irradiance levels (7.96 W/cm^2, 15.92 W/cm^2 and 25.47 W/cm^2) with different duration times (10s, 5s and 3s respectively) were applied on incisions as pointed out in Figure 4.1. Liquid solder mixture was dropped with micropipette (200 μl) to one incision which belong to corresponding power group. Each power level and solder application was ensured in any of these incisions.

Surgical and post surgical procedures were explained in Methods part. Rats has been followed for 4-day healing period. Tissue processing and staining procedures were done according to mentioned anywhere in this thesis. H&E stained samples were examined under light microscope to quantify thermal effects of laser application over skin tissue. Thermal width and depth, coagulation and carbonization were inspected [93].

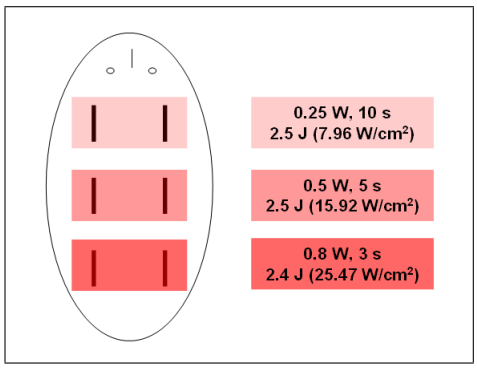

Figure 4.1 Laser groups. 3 pairs of incisions were made parallel to spinal cord and closed 809-nm laser with and without solder. Group A: 0.25 W power applied 10 seconds 7.96 W/cm^2, Group B: 0.5 W applied 5 seconds 15.92 W/cm^2, Group C: 0.8 W applied 3 seconds, 25.47 W/cm^2. 200 μl solder material (2.5 mg/ml ICG + 25% BSA (w/v)) was dropped on each incision of one incision of each group before laser application. Each irradiance application either soldered or welded was tried on every time in different incisions made on dorsal skin of six rats that was six different incisions.

4.1.3 Macroscopic Results

Operated areas were photographed everyday during healing period whether there was any openings of welded and soldered incisions, or any change in dietary habits of animals followed. In welding application, four of six incisions at 7.96 W/cm^2 irradiation, one of six incisions at 15.92 W/cm^2 and 25.47 W/cm^2 irradiances were opened after operation. On the other hand, in soldering application, two of six incisions at 7.96 W/cm^2 irradiation were opened. No opening was observed for both 15.92 W/cm^2 and 25.47 W/cm^2 irradiances for soldering group. Figure 4.2 reveals macroscopic results on Day-4.

4.1.4 Microscopic Results

Histological examination shows that 809 nm laser welding and soldering were not able to full dermal closure of incisions after 4-days of healing period (Figure 4.3). Thermal damage was observed in both methods. Dermal thickness increased in welding application, epidermis melted and fused with soldering material in soldering application. Macrophages become abundant around soldering material (Figure 4.3). Incisions' edges attached to each other because of hardened albumin during 809 nm laser irradi-

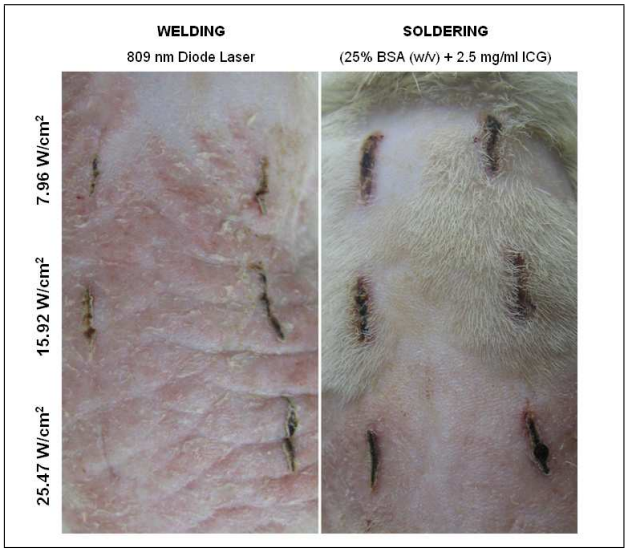

Figure 4.2 Macroscopic view of welded and soldered incisions after 4-day healing period. During this period rats were kept in different cages to prevent biting of animals each others lesions. In both group, epidermal scab which is more apparent in welded group was formed because of itching themselves.

ation. How this formation affects healing should be investigated during 21 day healing period.

4.1.5 Image Analysis

Qualitative and quantitative gross histopathological studies of skin thermal damage were performed 4 days after irradiation with 809 nm diode CW laser to compare the effects of welding and soldering of this wavelength. Histological sections were studied; for each applied parameter, widths and depths of thermal effect were measured. Damage is measured and documented using 809 nm diode laser powers around threshold values depending on literature. The data provides experimental evidence of the correlation of histological change to visible threshold anastomosis for the irradiation condition.

Soldered samples' thermal width was found wider for 25.47 W/cm^2 power density *($p<0.05$)*. On the other hand, welded samples' thermal diameter was found wider for 15.92 W/cm^2 power density *($p<0.05$)*. Welded incisions thermal depth were deeper than soldered ones for 15.92 W/cm^2 application *($p<0.05$)*. In Figure 4.5 thermal effects

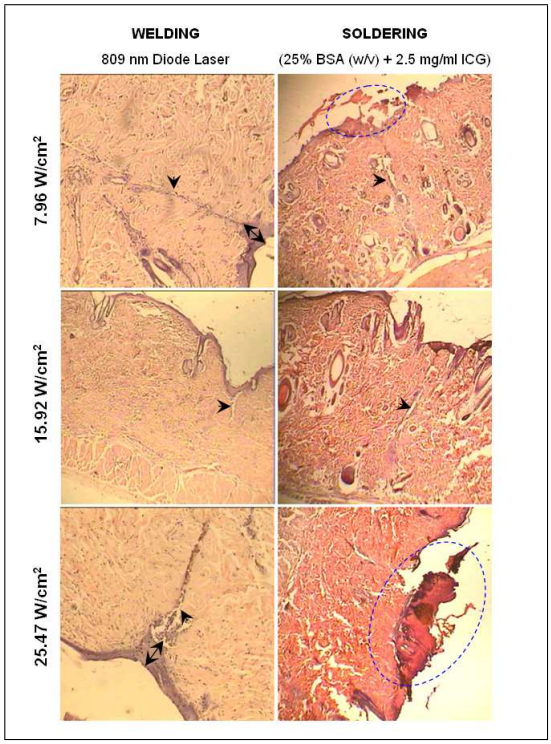

Figure 4.3 Microscopic view of welded and soldered incisions after 4-day healing period. Both methods cannot be able to full-closure of skin incisions (arrows) after 4 days. Remnants of solder material (blue circles) was still visible, cannot be digested by macrophages yet. Epidermal thickness increased in welded group (double-headed arrows).

are shown in graphics for soldered group and welded group.

4.1.6 Discussion

Laser tissue soldering (LTS) using a diode laser and an indocyanine green (ICG)/albumin solder has been shown to be an effective technique by providing watertight sealant with minimal damage to underlying tissue [85, 94]. Cooper *et al.* [87] tried power densities of 3.2, 8, 15.9, 23.9, 31.8, 47.7, and 63.7 W/cm^2 at constant ICG concentration (2.5 mg/ml). 15.9 W/cm^2 power density was found providing the most controlled heating curve. At a power density of 15.9 W/cm^2 or below, increasing ICG concentrations did appear to result in small, but significant, increases in immediate tensile strength as well. 15.92 W/cm^2 power density showed the optimal result in our study in a different aspect: thermal quantitative measurements. Results favored the 15.92 W/cm^2 power density in laser skin tissue soldering by giving less thermal

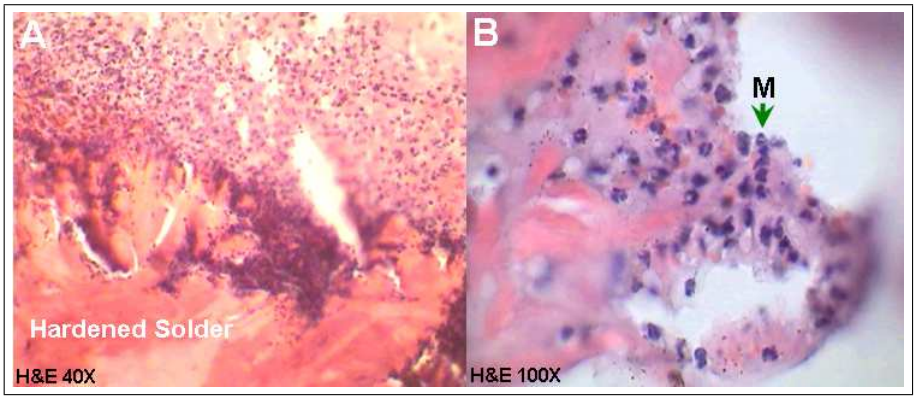

Figure 4.4 Macrophages around solder material. Albumin and ICG are biodegradable materials. This mixture can be digested by macrophage cells. Picture-A (X40) shows macrophage cells can not easily invade the solder material especially in the region that solder material is so stiff. High temperature caused solder material to become hardened. This may prolong the healing period. Picture-B (X100) shows invaded macrophage cells (arrow - M). Solder material was degraded and removed from incision site.

damage and higher closure rate. On the contrary, the results of the optimal parameter investigation performed by McNally et al. suggest that the strongest repairs are produced with lower irradiances of around 6.4 W/cm^2 after approximately 50 seconds exposure time by using a solid protein solder composed of 60% BSA and 0.25 mg/ml ICG on ex vivo aorta specimens [71]. Another in vivo study performed by Capon et al. [40] on mutant OFA Sprague-Dawley rats skin incisions closed over transparent adhesive dressing (Tegaderm, 3M Health Care, Borken, Germany) with the following parameters: 815 nm diode laser,1.5 W; 3 seconds; spot diameter: 2 mm; fluence: 145 J/cm^2. The parameters used in this study lead to a slow temperature increase up to a plateau below the critical coagulation temperature (53^{o}C$\pm$60^{o}C), avoiding thermal damage [46]. The optimal irradiance (47 W/cm^2) used in this study seems to be very similar to the value reported by Abergel et al. [95] (50 W/cm^2). Three times higher laser irradiance was applied for effective skin closure compared to current study without any thermal damage. High irradiation was avoided by use of ICG and use of albumin supplied good apposition for tissue closure.

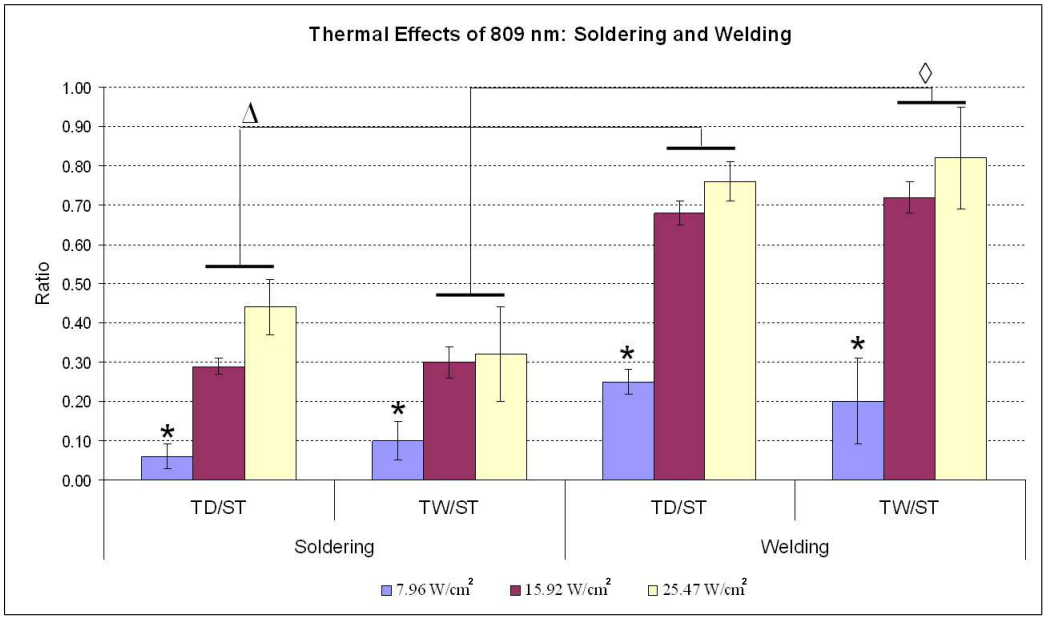

Figure 4.5 Thermal effects of soldering and welding applications were shown. Thermal width (TW) and thermal depth (TD) over skin thickness (ST) values of 7.96 W/cm^2 irradiance group were significantly ($p<0.05$) less than other groups, for soldering and welding applications (*). TD/ST (Δ) and TW/ST ($\diamondsuit$) of 15.92 W/cm^2 and 25.47 W/cm^2 welding irradiances was more than soldering ones ($p<0.05$). Skin thickness of different part of dorso of rat was measured in between 1.2 to 1.8 mm

4.2 980 nm LASER TISSUE WELDING

A 980-nm diode laser was proposed to be a welding laser in dermatology due to its optimal penetration in tissue by our group [96]. A study of dose determination was performed to find the optimal parameters that provide best welding with possible lowest energy application. Power in the range of 1W to 10W with different on/off durations (in the range of 250 to 1000 ms) was delivered to different incisions [97]. Macroscopic examinations showed that in 5 to 10-W-intervals the incisions were welded without reopening and carbonization. Within this power range, 6W for 400 ms was found to be the optimum parameter for welding without thermal damage to nearby tissue with the lowest energy density (0.76 J/mm^2) [96]. According to the results of this study, histological analysis revealed no significant differences between wound healing of laser-welded and sutured incisions after 21 days of full recovery period (Figure 4.6). Thermal injury was seen in the laser-welded wounds within the 24-h period; however, thermal alteration was not detected since the fourth day of recovery. Carbonization, which is a possible but unwanted effect of laser, was not observed in any of the welded incisions.

Better apposition was noticed in the laser group in the first 7 days compared to sutured cuts. Laser welding results in full-thickness close up, whereas suturing leads to healing from top to down starting from the epidermis and proceeding toward the deep dermis. Full thickness welding can also decrease the inflammation risk during healing.

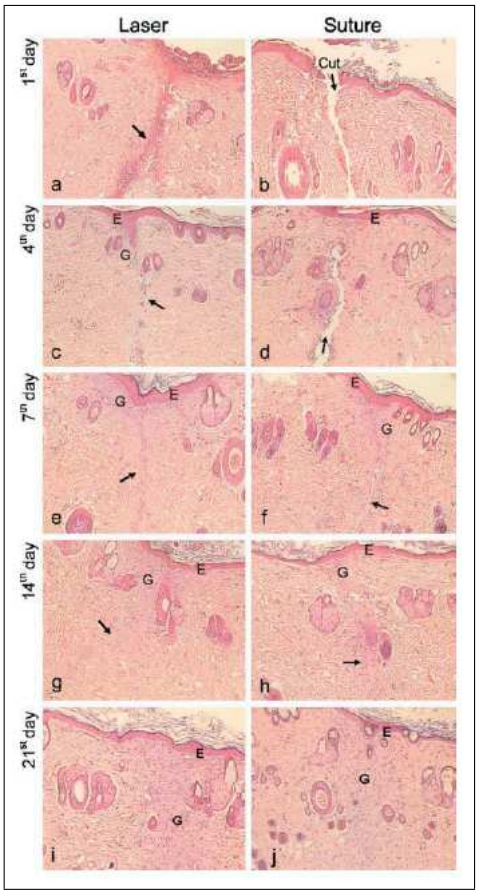

Figure 4.6 Light micrograph of paraffin embedded in 3-5 mm rat skin sections stained with standard histological examination (H&E staining).Arrows point out incision line along epidermis and dermis. Epidermal thickness (E) and granulation (G) sites are indicated on figures (x100).Laser welding results in full-thickness close up; on the contrary, suturing leads to a top-down healing starting from epidermis and proceeds toward the dermis. Thus, at day 7, opening in the dermis was observed for the sutured samples [96].

4.2.1 Dosimetry Study for Low Level 980 nm Diode Laser Irradiation

Same methodology was followed as in 809 nm dosimetry experiments. 6 male Wistar rats weighing 295-310 g were used. 1 cm long surgical incisions were made parallel to the spinal cord with no. 11 surgical blades. Different power levels (7.96 W/cm^2, 15.92 W/cm^2 and 25.47 W/cm^2) with different duration times (10 s, 5 s and 3

s respectively) were applied on incisions. No external chemical or biological agent (like solder) was applied.

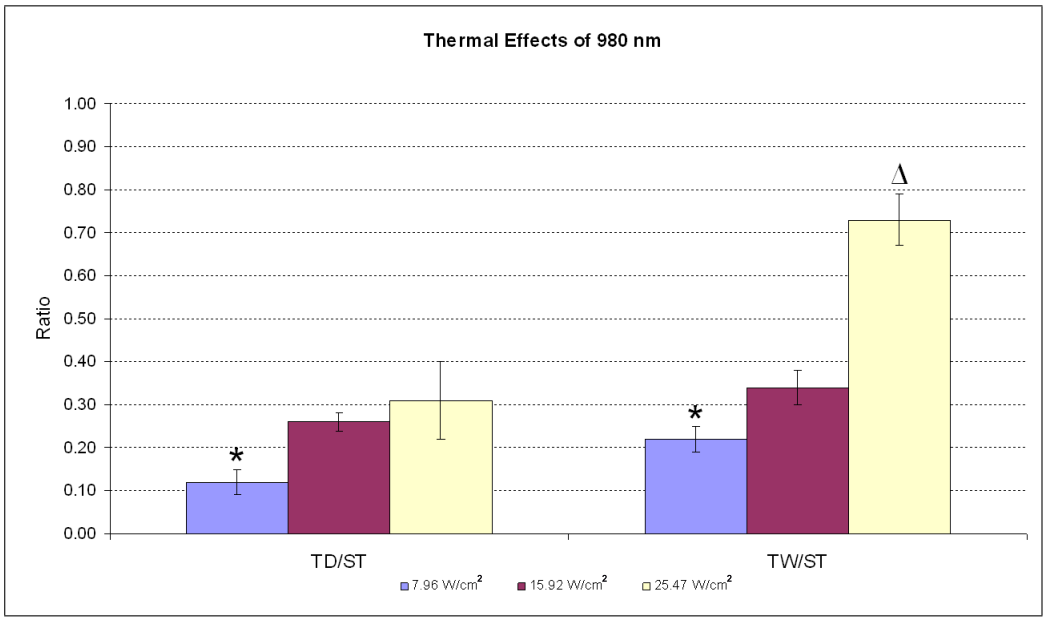

Figure 4.7 Thermal effect of 980 nm welding at low level irradiances was shown. Thermal width (TW) and thermal depth (TD) values of 7.96 W/cm^2 irradiance group were significantly ($p<0.05$) less than other groups (*), TW/ST ratio of 25.47 W/cm^2 welding irradiance was significantly more than TD/ST ($p<0.05$) ($\triangle$). Skin thickness of different part of dorso of rat was measured in between 1.2 to 1.8 mm

4-day histological evaluations were summarized in Figure 4.7. Birefringence change of tissue and H&E staining gave illustrative information on thermal effect on tissue. Low level 980 nm laser applications invade up to 30% to 40% of dermal depth. On the other hand thermal effect spread about 70% to 80% superficially (25.47 W/cm^2 - 0.8W-3s). All incisions closed except five of twelve irradiated by 0.25 W for 10 seconds (7.96 W/cm^2). No carbonization was observed in any cases. 5 W - 5s (15.92 W/cm^2) parameter was chosen for comparative study of HI and LI application of 980 nm diode laser.

4.2.2 The Effect of Irradiance Level in 980 nm Diode Laser Skin Welding

If photothermal laser applications concern, different laser modalities on tissue results in different tissue response such as carbonization, coagulation, hyperthermia [98]. Optical and thermal properties of tissue under laser irradiation may change

severely when a certain point temperature level is reached. Due to dehydration of tissue, thermal conductivity decreases, in turn local temperature increases [44, 45]. Tissue welding with high laser irradiances can cause high heat deposition and sudden increase in temperature, thus cell necrosis and denaturation of structural proteins take place irreversibly [42, 62, 63]. Continuous high power applications may also result in thermal damage. In order to minimize the irreversible thermal damage the time interval between subsequent laser pulses must be greater than the thermal relaxation time [2]. In low power applications, on the other hand aimed results may not be obtained due to insufficient temperature increase. Long exposure times might be needed to achieve closure of the tissue. To focus required energy to the target tissue portion, various kinds of soldering agents were tried in combination with appropriate wavelength. Stronger welds were achieved but introducing of any soldering agent, either solid or liquid to the wound has some sort of inconsistencies and difficulties. Infrared lasers have been under investigation for decades. CO_2, Ho:YAG and Er:YAG lasers are absorbed within 2-20 μm at the surface of the tissue and may cause unwanted thermal hazards at long exposure times and high power applications. For this reason different kinds of temperature control systems have developed. Conversely, diode lasers irradiated around 800 nm and 1064 nm Nd:YAG lasers can penetrate into deeper layers. In this spectral region of interest, 980 nm wavelength was proposed as an alternative for skin welding studies due to its relatively optimal penetration to the tissue because of relatively higher absorption by water (H_2O-μa = 0.43 whereas H_2O-μa is 0.023 and 0.12 for 810 nm and 1064 nm respectively) (Figure 4.8) [99, 100]. In this study, optimal doses of high and low irradiances of 980 nm diode laser were examined with reference to sutured incisions for skin welding *in vivo* both histological and mechanical point of view [101, 102].

4.2.3 Experimental Design

980 nm Diode Laser System, suturing technique, surgery and post surgical operations was mentioned in Materials and Methods chapter. A total of 60 healthy male Wistar rats (30 for histological and 30 for tensile strength tests), randomly selected, 6-9 months old, weighing 295-310 g, from Psychobiology Laboratory of Bogazici University

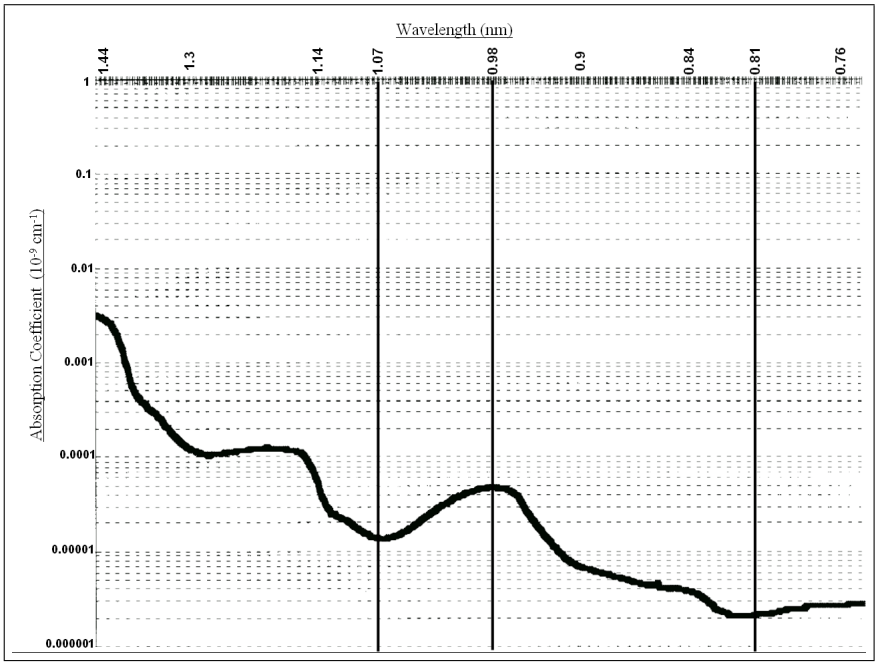

Figure 4.8 Absorption coefficient of water with respect to wavelength between 1.44 - 0.76 μm [96].

were used. 6W for 400 ms per spot was chosen as the optimum dose for high irradiance (200 W/cm^2) from previous study [96]. 0.5W for 5s per spot was set according to a series of predosimetry experiments as optimum dose as low irradiance (15.92 W/cm^2). These parameters were applied for this comparative study to evaluate the performance of the welding process with respect to suturing technique (Figure 4.9). At the given power, pulse duration and number of spots per incision, the resulting total energy was 14.4 J per incision. The radiant exposure was 0.76 J/mm^2. Three of six incisions in each of rat were closed with high irradiance (HI) and the other three wounds were welded with low irradiance (LI). HI and LI were randomly distributed among incisions. No suture was placed any of the rats incisions closed by 980 nm laser to avoid any possible mechanical opening of laser closed incisions during suturing. The wounds on the rats were examined and photographed daily during the recovery period. Presence of wound reopening, infection, scar and hair formation was checked on a daily basis. In comparative study, recovery period was observed through 21 days.

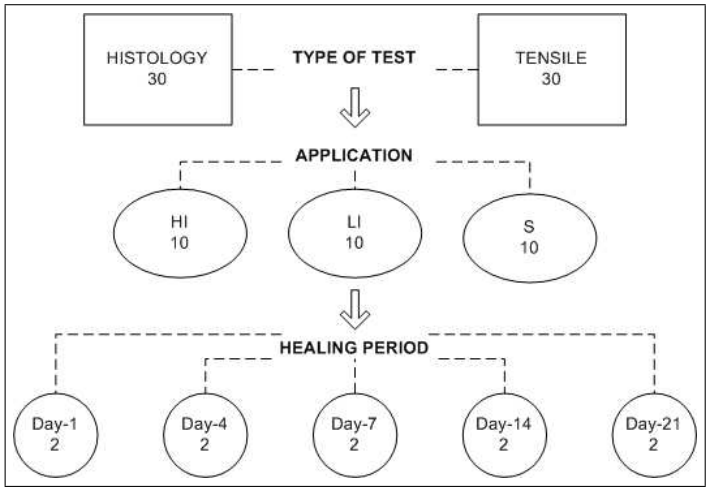

Figure 4.9 Organization Chart for 980 nm Irradiance Level Effect on Skin Tissue Experiment. HI: High Irradiation, LI: Low Irradiation, S: Suture

4.2.4 Histology Results

H&E stained sections were studied on particular post-operation dates under microscope for general histology (Figure 4.10). In all groups, mild inflammation and similar foreign body giant cells was observed in very early days of wound healing within the dermal tissue due to hair follicles that burst during the procedure of skin cutting, laser welding, and suturing or suture material itself . On Day-1, incisions were inspected as closed tightly at skin surface with welding applications but thermal hazard was observed for HI applications. No closure (NC) was noted in sutured incisions and at the wound site neutrophils leukocyte accumulation was observed. On Day-4, perivascular inflammation with neutrophils infiltration was noted in HI and LI groups' samples. For laser welding groups, contraction was observed on the surface layer tightly and almost closed in full thickness but in some samples of HI group, necrotic detachment was observed between stratum germinativum and papillary dermis as well as macrophage activity. At the laser spot site, hyperkeratosis in the epidermis was observed also in HI group. On the other hand, only basal epidermal layer and papillary were closed in sutured samples and deeper parts of the incisions was remained open. On Day-7, full thickness closure was noted for all groups. Hyperkeratosis was observed in LI and suture group. Muscular layer was incised infrequently. Ablation crater was still observed on HI group. Necrotic detachment was seen some of samples in suture

group. After Day-14, no difference was observed within groups. In the papillary and reticular dermis, wounds were narrowed to a fine scar. The visibility of the scar tissue had decreased. The epidermal hyperplasia was decreased and the epidermal thickness reached to normal levels. Knot openings were observed rarely in suture group samples. Besides those general observations, microscopic images were analyzed quantitatively in terms of closure index, thermally altered tissue area, granulation area and epidermal thickness values in order to quantify the closure quality.

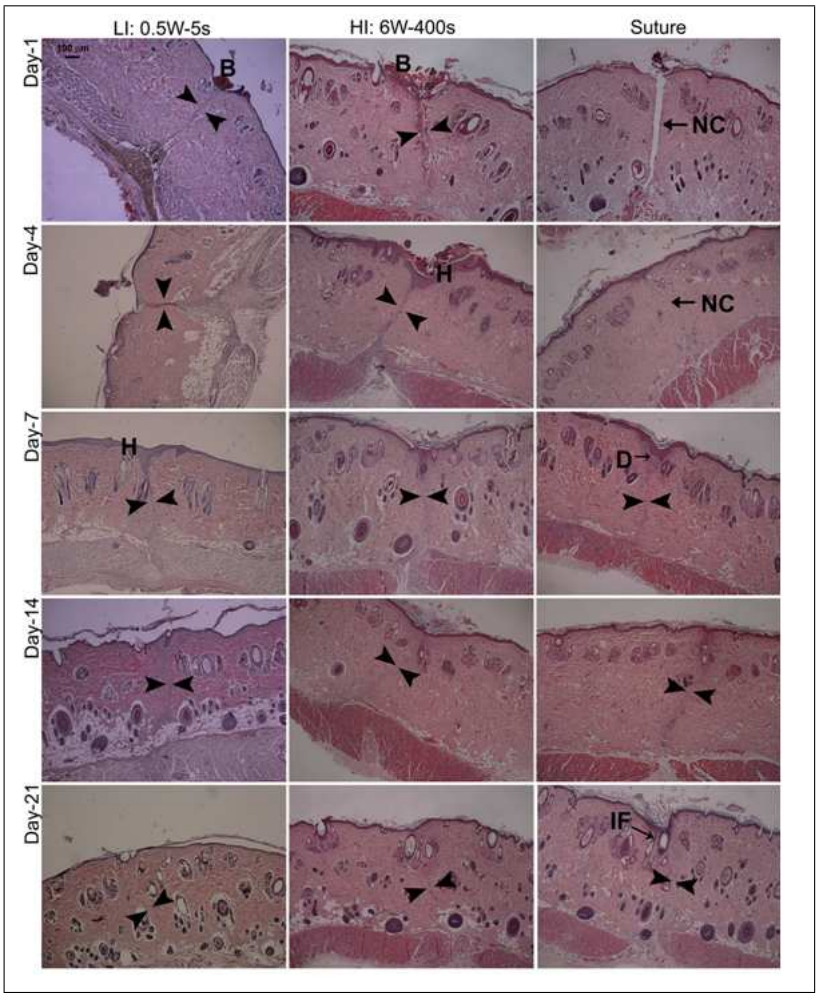

Figure 4.10 Microscopic view of incisions closed with laser welding high irradiance (HI) (200 W/cm^2), or low irradiance (LI)(15.92 W/cm^2), or suturing (S), on particular control days. On day 1, epidermal and upper dermis ablation was noted in the HI and LI groups. Although removed totally before laser applications, blood (B) remnants were observed on top of welded incisions. The degree of non-closed (NC) parts in sutured incisions on days 1 and 4 was observed more clearly in micro inspection. Incision lines were marked on photographs taken during the healing period using face to face arrowheads. Hyperkeratosis (H) was marked on the HI sample, day 4, and LI sample, day 7. Necrotic detachment (D) and inward folding (IF) were observed in some sutured samples. The course of healing after day 14 postoperative seemed to be similar for all experimental groups microscopically.

On Day-1, in suture (control) group, there was no closure 24 hours after surgery (CI=0.00) ((Figure 4.11). For laser groups, immediate closure at the surface layers of the incisions was observed: High irradiation of 980 nm laser resulted immediate closure on the surface of the cut and almost half thickness (from surface to deep dermis) welding was achieved (CI=0.44±0.22); low irradiation of 980-nm diode laser (CI=0.28±0.08) also had immediate closure on the surface.On Day-4, HI group closure was 0.70±0.36, and LI group closure was 0.39±0.05 and they were statistically different (*) ($p<0.05$). Sutured incision closure (0.12±0.09) was statistically less than laser welded groups (**) ($p<0.05$).

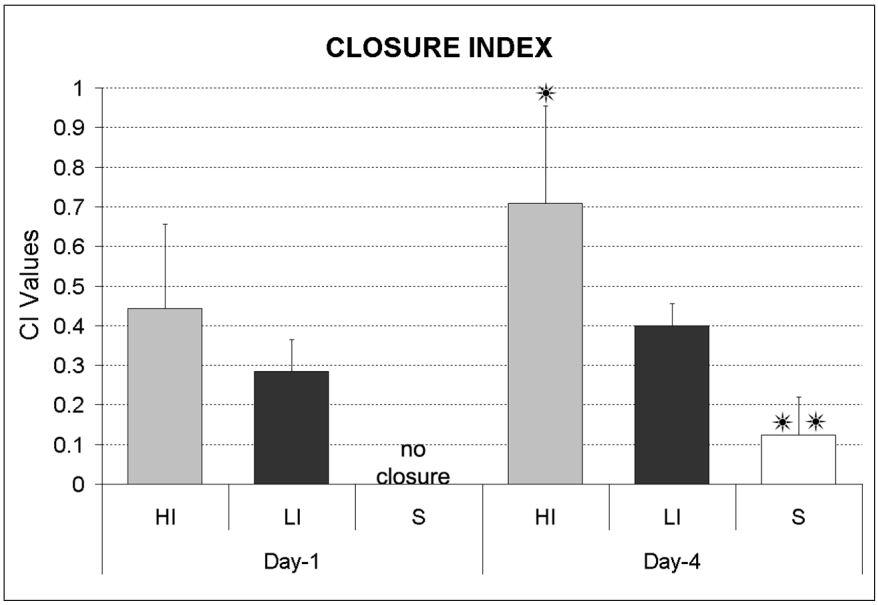

Figure 4.11 Closure index values. Closure index (CI) is the ratio of closed segment to the total incision (from skin surface to subcutaneous layer). On day 1, laser welding modalities showed immediate closing effects, whereas sutured incisions remained open. On day 4, laser groups CIs were still significantly greater than for the suture group (**) ($p < 0.05$). HI group closure ability was higher on both days 1 and 4, but statistical significance was found only on day 4 (*). The number of samples was 12 for each group.

Early response of laser irradiated tissue to photothermal interaction was observed in 1st and 4th post operative days (Figure 4.12). On Day-1; HI group thermal areas (386472±68974 μm^2) were statistically higher than LI group (159548±54461 μm^2) ($p<0.05$). On Day-4; TAA significantly narrowed to 129548±42195 μm^2 for HI group and to 48962±21476 μm^2 for LI group. HI group had also statistically higher thermal hazard than LI group ($p<0.05$).

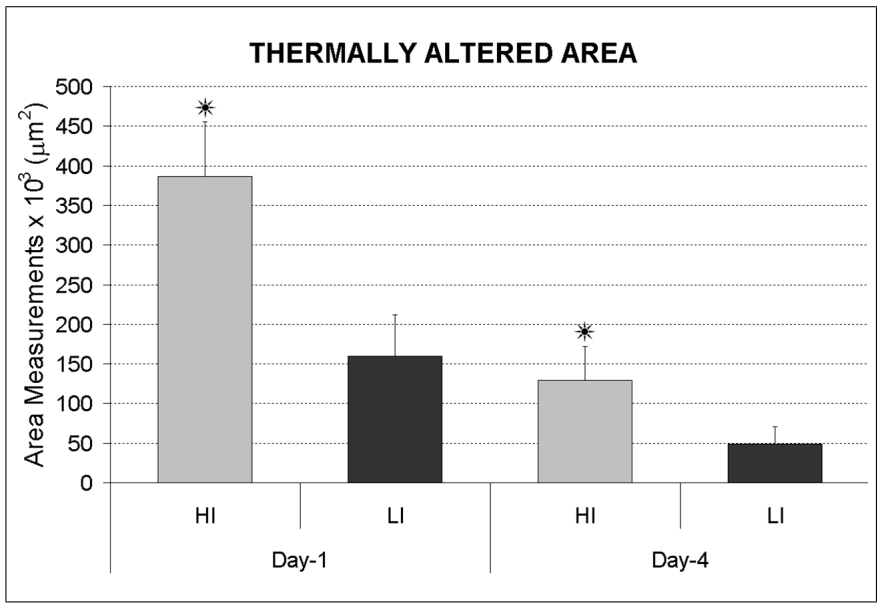

Figure 4.12 Thermally altered areas. High thermal damage of HI group compared to LI group was observed on early recovery period (*) ($p<0.05$). Number of samples was 12 for each group.

Granulation tissue has started to be clearly inspected 7th post operative day and no statistical difference was found either of groups (Figure 4.13). HI group granulation was statistically different from both LI and control (suture) groups on Day-14 and Day-21 (**). LI and suture groups granulation tissue have stayed around the same level (150x103 - 200x103 μm^2 and 200x103 - 300x103 μm^2 respectively).

Epidermal thickness measurement was started on 4th post operative day to make robust assessment (Figure 4.14). On Day-4; thicknesses were measured as, for HI group 76.26±13.81 μm, and LI group 45.81±13.97 ($p<0.05$) (*). Welding results were statistically less than the control group (113.40±20 μm) ($p<0.05$) (**). On Day-7; HI group was measured 113.17±16.66 μm and LI group was measured 84.43±13.14 μm (*)($p<0.05$). Suture group (87.40±27.10) was not statistically different from welded incisions epidermal thicknesses. On Day-14; HI group ET was measured 40.44±17.90 μm and LI group ET was measured 36.27±14.21 μm which statistically less than control group (*) ($p<0.05$). On Day-21; epidermal thickness was around 30-40 μm for all groups.

24 Hour post operation, tensile test result for HI group was 1.93±1.18 N while

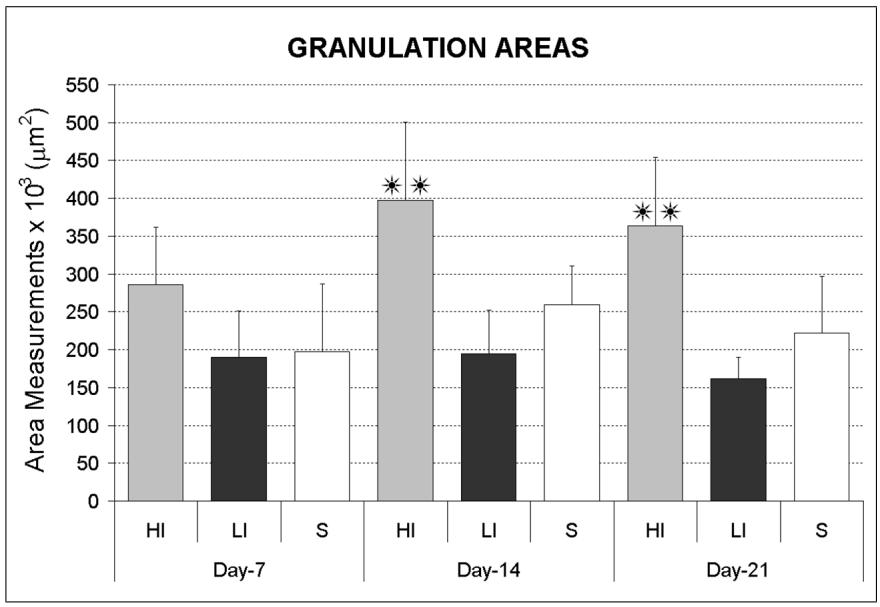

Figure 4.13 Granulation areas. High granulation was observed due to thermal hazard of the HI of the 980-nm diode laser on days 14 and 21 (**) ($p<0.05$). The number of samples was 12 for each group.

4.97±0.87 N for LI group which was significantly higher (*) ($p<0.05$) (Figure 4.15). Tensile strength was not measured for sutured incisions on Day-1 (incisions were not closed). On Day-4; HI group and suture group average tensile strengths were 3.73±1.63 N and 1.64±0.37 N respectively. LI group average tensile strength was 6.32±0.99 N which was significantly stronger than both HI and Suture (control) groups (**) ($p<0.05$). On Day-7; sutured samples tensile strength was 3.06±0.64 N. HI and LI groups tensile strengths were 5.65±1.26 N and 7.71±2.87 N respectively and higher than control group (**) ($p<0.05$). On Day 14; no statistical difference was observed among groups (tensile strengths were around 7-8 N). At the end of the recovery period (Day-21), LI group tensile strength was found to be the most persistent (15.7±1.95 N) (**) ($p<0.05$) compared to HI group (11.0±2.49) and suture group (9.17±2.28).

Although rat skin wound healing does not perfectly simulate human conditions, tissue welding and soldering studies were widely done rat models in order to examine the laser-tissue interaction [56, 103-105] Laser welding puts forward less bleeding, shorter operation time, reduced suture and needle trauma, however it does not find wide areas of applications in the clinical practice due to several major difficulties of the technique, lack of consistency, and unexpected thermal damage given to nearby tissue.

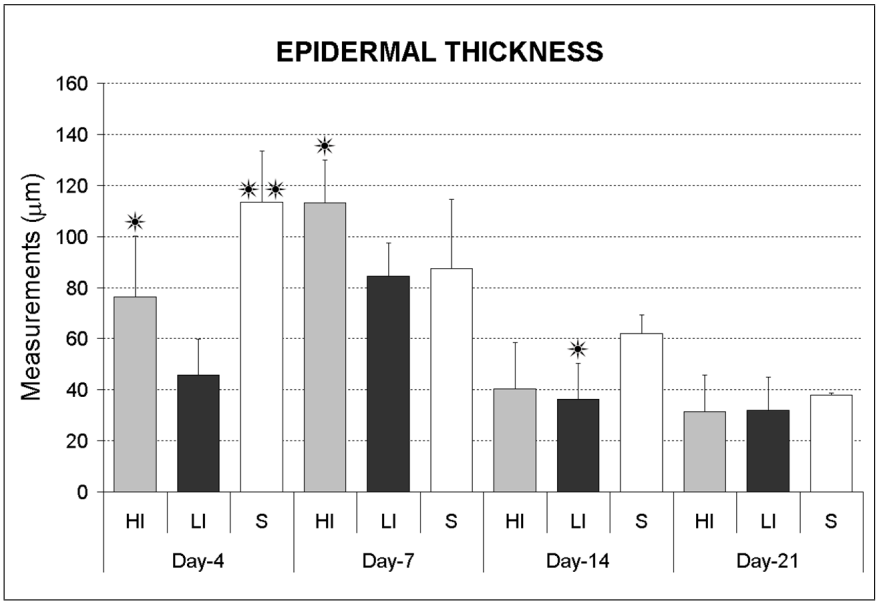

Figure 4.14 Epidermal thickness. No difference was observed at the end of the 21-day recovery period. The number of samples was 12 for each group.

Wound healing without thermal damage was aimed in the present study with low and high irradiances by assisting skin closure with a 980 nm diode laser. Macro inspection of 21 days wound healing period revealed data about the possible abnormalities around the incision site such as infections and thermal damages. Recovery of incisions was monitored on daily basis. No infection was inspected at neither of the groups, however, for suture group incisions were remained open, and this might be a potential for infections. The incision site was not flat and incision lines were irregular and deep for most of the sutured samples. Besides, openings along incision line and openings of needle entrances on both sides were also visible at early recovery days. Those negative outcomes were reduced in laser irradiated tissue such that, full superficial closure was achieved in both laser delivery types (Figure 4.10).

Histology of the H&E stained samples provided detailed observations supporting the macro inspections of recovery period. No carbonization was noted in welding applications which was verified at microscopic scale. The closing ability of appropriate irradiance levels was determined through well defined parameters and thermal alterations were described quantitatively: significant differences due to irradiance levels were reported although same amount of energy (2.5 J) was transferred. Closure rate

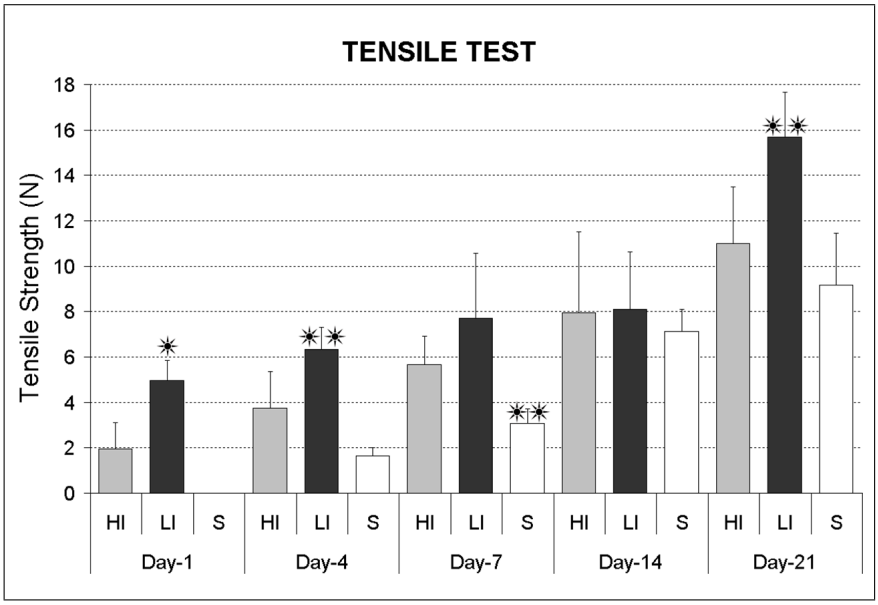

Figure 4.15 Tensile-test results. LI samples' tensile strength was higher in the early healing period, days 1 and 4, (*) (**) ($p<0.05$). On day 7, suture group samples were weaker than welded samples (**). The strongest closure was obtained with the LI welded incision at the end of 21-day recovery (**) ($p<0.05$). The number of samples was 12 for each group.

of HI group was higher than LI group, but side effects were more pronounced: higher thermal damage (not carbonization) which was realized in necrotic cell observation, increase of epidermal thickness (≈ 110 μm) on Day-4 and more importantly high granulation (≈ 400000 μm^2) even on Day-21. Low irradiance did not create as much heat as the HI at the target site. Thus LI case was found more suitable in terms of minimal thermal damage. These inferences were sustained by tensile test results. Although HI group has higher closure rate, mechanical tensile strength was lower than LI group in the first week post operation, especially on Day-1 and on Day-4 which were critical for wound healing. Remarkably, LI welded incisions on Day-1 were found stronger than the Suture group on Day-7. Not only in early period but also towards the end of the healing period, LI group tensile strength was found the highest (Day-21). Under LI conditions, less ET, less TAA, higher TS were achieved.

4.3 1070 nm LASER TISSUE WELDING

Objective of the study was to test welding ability of 1070 nm Ytterbium Fiber Laser (YLF) *in vivo* which has not been examined before. (For description; Single Mode CW Ytterbium Fiber Laser developed for use in spectroscopy, medical research and industrial applications. These lasers are compact and efficient allowing them to replace bulky and less efficient lasers. Fiber lasers confine the pump light and the stimulated emission to small volumes, allowing pumping efficiency to exceed 80% in the best materials. Pumping with high-power diode lasers, therefore, can effectively convert low-quality diode output into powerful, high-quality beams from the fiber laser)

Fiber lasers have been developed recently. This is a laser in which the active gain medium is an optical fiber doped with elements such as erbium, ytterbium, neodymium, and thulium. They are promising lasers for medical application, with high output power and compact size. No tissue welding with a 1070 nm fiber laser has been reported as yet. However, results similar to those with a 1064 nm neodymium:yttrium-aluminum-garnet (Nd:YAG) laser can be expected, since the optical properties of tissues do not change drastically within that narrow range. Penetration of a collimated 1064 nm light beam in soft, non-pigmented tissue such as a vessel wall or albino skin is approximately 1.5 mm [44]. Moreover, optical penetration with a 1,064 nm wavelength into human mucous tissue was found to be approximately 5 mm [106]. Fried et al. explained that the reason for choosing the Nd: YAG (1064 nm) laser for skin welding was to achieve the deep penetration of radiation and, therefore, deep heating at the weld site, which is necessary to produce strong, full thickness skin welds [52].

In a study that Nd:YAG (1064 nm, CW) laser skin welding have been performed by Fried *et al* [52] which is very close to 1070 nm was found that scanned delivery of near infrared laser radiation in combination with a dye can produce strong welds with limited thermal damage. Two-centimeter-long, full thickness incisions on the backs of guinea pigs were closed either by laser welding (10W) or sutures and then biopsied at 0, 3, 6, 10, 14, 21, and 28 days postoperatively. Welding was achieved by laser radiation (laser spot was 4 mm diameter) scanned over the incisions to produce a dwell time of

80 msec waiting 8 seconds for tissue cooling between scans. The operation time was 10 minutes per incision. Tissue edges was apposed by clamps and India ink was used as an absorber of the laser radiation at the weld site. The welds were created and endured without the aid of sutures, biological adhesives, or chemical cross-linking agents, and healed without dehiscence or excessive scarring in guinea pigs.

Six millimeter full-thickness incisions made on backs of hairless mice were closed by 1064 nm Nd:YAG laser operated at 1W (50 W/cm^2) [95]. Cosmetic appearance of laser-welded wounds was significantly better than in sutured wounds: suture tracks present in the suture closed wounds were absent from the laser-welded wounds.

In this part of study, 1070-nm Ytterbium Fiber Laser (IPG Laser GMBH, Model: YLM-20-SC, 20 Watt optical power, Class IV Laser) was used for skin welding without any soldering agent [107]. Same methodology was applied as in 980 nm low level irradiance dosimetry study. Three different power levels and time durations (0.25W-10s, 0.5W-5s, and 0.8W-3s) were applied on incisions. Surgery, laser delivery and histology were described elsewhere in this thesis. Histological examination was made in order to understand thermal damage and degree of welding of 1070 nm YFL.

4.3.1 Macroscopic Results

Macroscopic results of 4 days recovery period have shown no difference. No opening in any of the experimental group was noted after surgery.

4-day histological evaluations were summarized in Figure 4.17. Low level 1070 nm laser applications invade up to 70% to 75% of dermal depth. On the other hand thermal effect spread about 20% to 30% superficially (25.47 W/cm^2 - 0.8W-3s). All incisions was closed successfully by any of irradiance levels. No carbonization was observed in any cases.

Up to this point, thermal-safe power levels was set for each of the NIR lasers

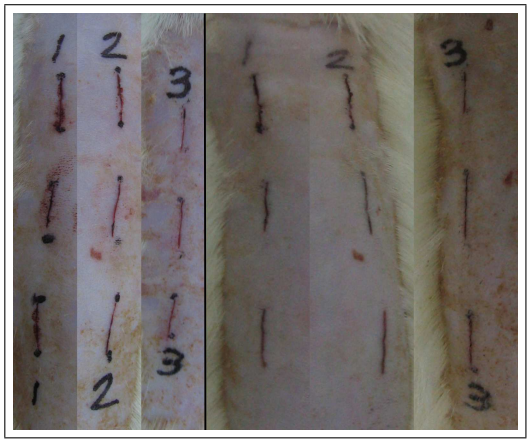

Figure 4.16 Macroscopic view of 1070 nm YFL welded incisions. After surgery, tissue welded successfully. On the fourth day, tissue closure shows no difference between groups

for skin tissue welding depending on histological results. In addition, high and low irradiations of 980 nm diode laser was compared mechanically. In the next section, these three NIR lasers will be compared; all has same irradiance level: 15.92 W/cm^2.

4.4 *In vivo* COMPARISON OF NEAR INFRARED LASERS FOR SKIN WELDING

Various kinds of infrared lasers have been manufactured between 700 nm and 11000 nm for the past decades. Among them, diode lasers can be produced in diverse wavelengths, especially in the spectral region between 800 nm and 1100 nm [108]. The effect of near infrared lasers has been investigated on different tissues such as skin, nerve, heart, urinal tissue [2]. The dynamics of the skin's optical and thermal processes in the near infrared spectrum, as well as the wound healing of laser-irradiated tissues have been examined for years [47,52]. In our study, three near-infrared lasers (809 nm, 980 nm and 1070 nm) and the conventional suturing technique were compared with respect to their skin closure abilities during a 21-day recovery period on dorsum skin of Wistar rats. The laser parameters except wavelength were kept constant, and the results were inspected by histology and mechanical tests in order to detect thermal damage, which are the bottleneck of laser welding [59, 109].

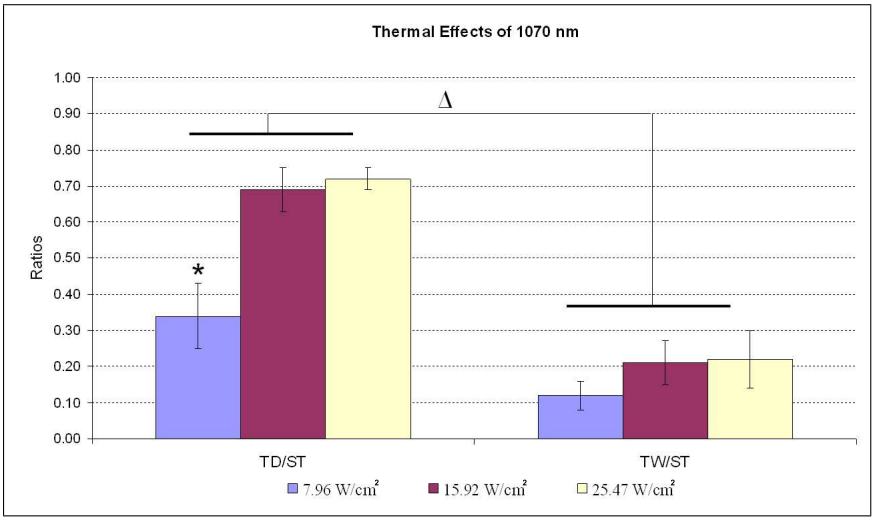

Figure 4.17 Thermal effect of 1070 nm welding at low level irradiances was shown. Absorption has taken place at deep dermis (△). TD of 8W/cm^2 group was less than other groups. Skin thickness of different part of dorso of rat was measured in between 1.2 to 1.8 mm

4.4.1 Experimental Design

In all laser applications, 0.5 W of power was delivered to the tissue in 5 s continuously, resulting in 79.61 J/cm^2 energy density (15.92 W/cm^2 power density) for each spot. This dose was set according to a series of pre-dosimetry experiments reported previous sections in this thesis. The soldering material was a mixture of bovine serum albumin (Fluka-BioChemika, Fraction V, Buchs, Switzerland) and indocyanine green (Pulsion Medical Systems AG, Munich, Germany). The soldering solution was composed of 25% BSA and 2.5 mg/ml ICG and was used as a soldering agent only for 809 nm application. Two hundred microliters of ICG-albumin solder was dropped into the incision and spread as evenly as possible before the application of 809 nm diode laser. Solder or any blood remnants were removed from the skin surface so that radiant energy was focused and absorbed inside the incision. The recovery process was followed up for 21 days. The 1st, 4th, 7th, 14th, and 21st days of this period were determined as control days, and skin samples needed for histology and tensile tests were removed on these particular days (Figure 4.18).

For histological examinations, 40 Wistar rats (ten from each group: 809 nm, 980 nm, 1070 nm and suture) were anesthetized with ketamine, and 2 cm x 1 cm pieces of

skin containing 1 cm long incisions were removed. Any histological change was followed by H&E staining on tissue samples. Tissue healing parameters (CI, TAA, GA and ET) were quantified as described.

For tensile tests, 40 Wistar rats (ten from each group: 809 nm, 980 nm, 1070 nm and suture) were anesthetized with ketamine, and the incision sites were removed as dumbbell-shaped stripes approximately 5 cm long. The sutures were removed on the 5th post-operative day, which is suitable for removal of the knot of healed tissue [103] to allow measurement of the mechanical strength on days 7, 14 and 21. Tensile strengths were tested fewer than 10 min after the removal, to minimize drying.

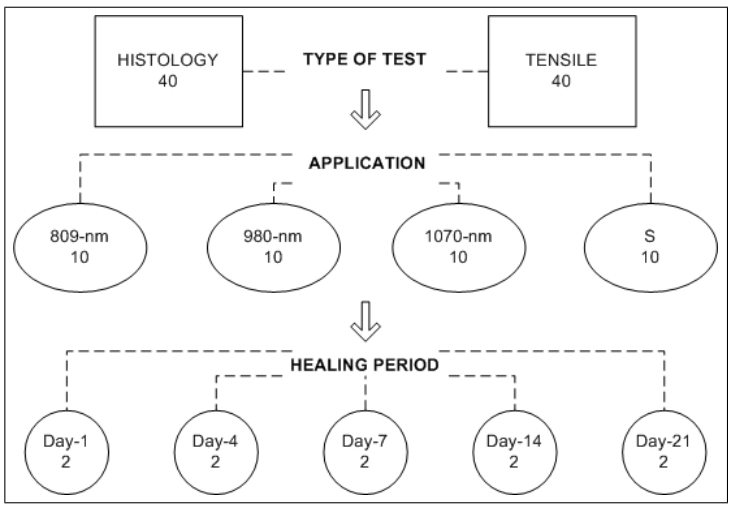

Figure 4.18 Organization Chart for comparison of near infrared lasers for skin welding experiment.

4.4.2 Macroscopic Results

Healing of the incisions was monitored on a daily basis, and the incisions were photographed on the post-operative control days (Figure 4.19). On day 1; moderate thermal damage was observed in the groups subjected to 809 nm and 980 nm laser. No damage was detected in the group irradiated with 1070 nm laser. No infection was found at neither of the groups. However, in the group that had undergone suturing, the incisions remained open, and this might have been a potential for infection.

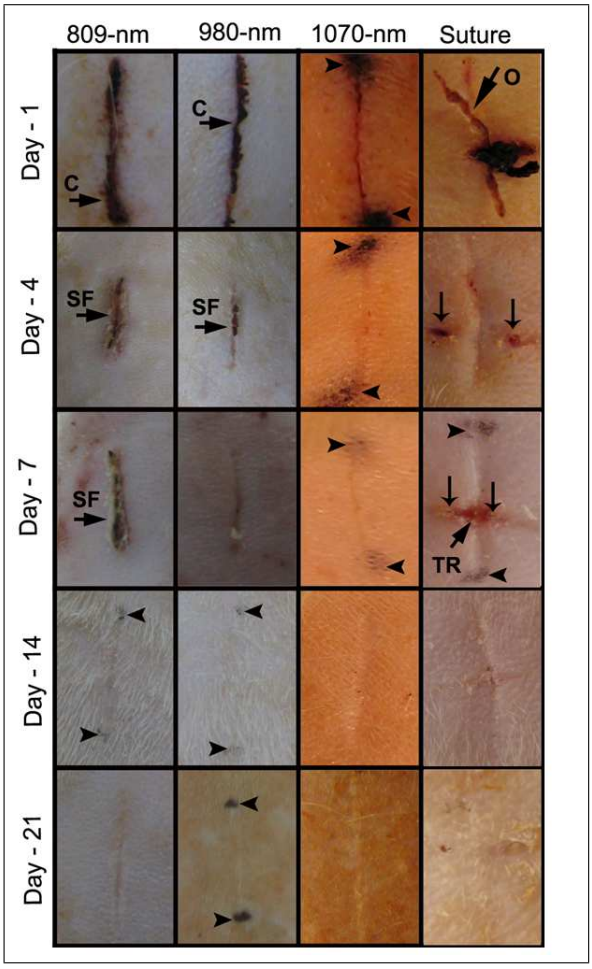

Figure 4.19 Macroscopic views of the incisions, closed by either laser soldering (809 nm) or laser welding (980 nm and 1,070 nm), or by suturing, on the control days. On day 1, charring was observed on both the 809 nm soldered and 980 nm welded incisions (C). Sutured incisions had opened up (O). The 1070 nm welded incisions had closed well. In some photographs, the end points of the incisions are marked (arrowheads). Scab formation (SF) was noted on day 4 on the 809 nm soldered and 980 nm laser welded incisions. Tissue reaction (TR) was noted in some sutured incisions (on day 7). Thin arrows point to needle holes in the skin on the 4^th and 7^th post-operative days

On day 4, gross scab formation was seen in the group subjected to 809 nm irradiation. Scab formation was also observed in the 980 nm group, but they were minimal compared to those in the 809 nm group. In the group irradiated with 1070 nm laser, no scab formation was recorded; the incisions were observed as clear thin lines. In the sutured group, the incisions were closed, but the incision site was not flat and the incision lines were irregular and deep in most of the samples. Additionally, openings along the incision lines and openings of needle entrances on both sides were also visible on the sutured incisions. On day 7; there were still scabs on the 809 nm soldered incisions. The groups subjected to 980 nm and 1070 nm laser were found to be

totally recovered, the incisions being thin lines. However, in the sutured incisions, the irregularities reported on day 4 were still visible. On day 14 and day 21, no differences could be identified macroscopically between the laser groups. All incisions had become very thin scars. Rarely, thin red scabs were detected in some rats' skins where they had scratched around the incisions. However, for the group that had undergone suturing, the needle and silk thread had caused a scar perpendicular to the incision site. On day 14 the incisions were found to be deeper than those in the laser groups, and, on day 21, the incisions of the suture groups were more visible.

4.4.3 Microscopic Results

Samples were taken for microscopic examination on the post-operative control days (Figure 4.20). On day 1, in the group subjected to 809 nm irradiation, besides the carbonization of solder material, much thermal damage was observed around the incisions. No (or negligible) thermal damage was observed in the 980 nm and 1070 nm laser-irradiated skin samples. The incisions were closed tightly at the skin surface for all laser groups. Conversely, no closure was noted in the sutured incisions, and, at the wound site, neutrophil leukocyte accumulation was observed. On day 4, in the 809 nm irradiated group, closure at the skin surface was not flat; epidermal layers had not stuck to each other regularly. Specifically, carbonized or denaturized solder material filled the apposition crater. Perivascular inflammation with neutrophil infiltration was noted in the 809 nm and 980 nm irradiated samples. Healing by reepithelization was similar in both the 980 nm and 1070 nm irradiated skin samples; the incisions had closed tightly on the surface layer and had almost closed to full thickness, but, in some samples, necrotic detachment was observed between the stratum germinativum and the papillary dermis. On the other hand, only the basal epidermal layer and papillary dermis had closed in the sutured samples, and deeper parts of the incisions remained open.

On day 7, full-thickness closure was noted in the 980 nm and 1070 nm groups. There were still small openings (2-3 μm) in the 809 nm-irradiated and sutured incisions

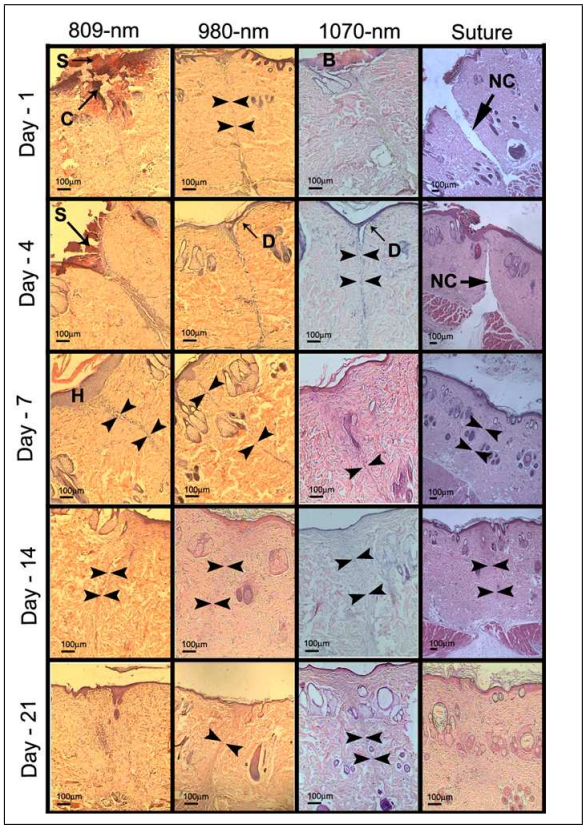

Figure 4.20 Microscopic view of the incisions, closed by either laser soldering (809 nm) or laser welding (980 nm and 1070 nm), or by suturing, on particular control days. Carbonized (C) solder (S) adhered to the tissue (day 1). Blood (B) remnants were observed on top of the 1070 nm welded incisions. The condition of the non-closed (NC) parts of the sutured incisions on day 1 and day 4 were observed more clearly on micro inspection. The incisions are marked on the photographs, taken throughout the healing period, with face to face arrowheads. Hyperkeratosis (H) was marked on the 809 nm (day 7) soldered wound. Necrotic detachment (D) was observed on the 980 nm and 1,070 nm welded incisions on day 4. Microscopically, the course of healing after the 14th post-operative day seemed to be similar in all experimental groups. H&E, X40 for the sutured group from day 1 to day 14;X100 for the remainder

along the reticular dermis. At the laser spot site, hyperkeratoses in the epidermis were observed in the 809 nm and 980 nm laser-irradiated samples as well. After day 14, no difference could be seen between groups. In the papillary and reticular dermis the wounds had narrowed to fine scars. The visibility of the scar tissue had decreased. The epidermal hyperplasia had also decreased, and the epidermal thickness had reached normal width and depth. Besides those general observations, microscopic images were analyzed quantitatively in terms of CI, TAA, GA and ET values so that we could determine closure quality.

4.4.4 Closure index

The immediate response of tissue is crucial in laser-welding techniques. The ideal welding process must create immediate full closure with little thermal damage. Thus, histological examination in the early phase (day 1 and day 4) of the recovery period revealed significant success for the technique Figure 4.21. In the sutured (control) group there was no closure 24 h after surgery (CI=0.00). In the laser-irradiated groups immediate closure (day 1) of the surface layers of the incisions was observed: 809 nm laser soldering with ICG resulted in immediate closure of the surface of the cut, and almost half-thickness (from surface to deep dermis) welding was achieved (CI=0.48±0.14); the 980 nm diode laser (CI=0.28±0.08) and 1070 nm ytterbium fiber laser (YFL) (CI=0.51±0.12) also produced immediate closure on the surface. On day 4, only partial closing was observed (CI=0.12±0.09) in the suture group; the laser groups showed significantly better closure ($p<0.05$), and there was no difference between laser groups. After 1 week of recovery, closure index values for all groups were 1.00; in other words, all the incisions had totally closed except for minor openings (2-3 μm) observed in sutured incisions and laser-soldered incisions along the dermis on the 7^th day. On day 14 and day 21 there was no opening in any of the groups.

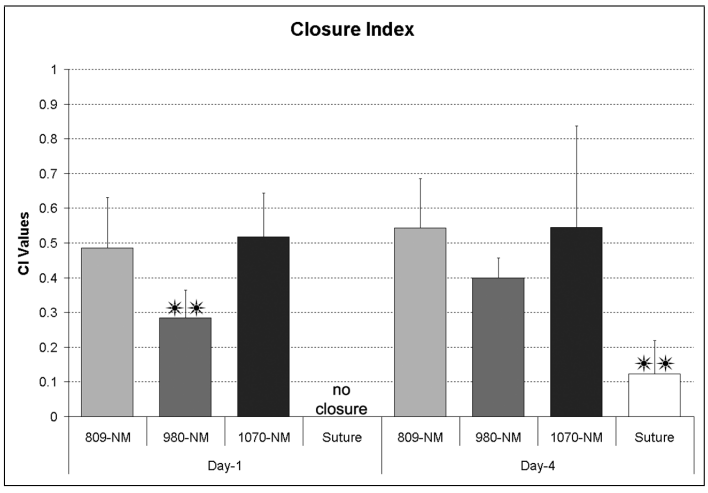

Figure 4.21 Closure index values of near infrared laser (809 nm, 980 nm, and 1070 nm) irradiated and sutured incisions. CI is the ratio of closed segment to total incision (from skin surface to subcutaneous layer). On day 1, all laser welding modalities showed immediate closing, whereas sutured incisions remained open; additionally, the 980 nm closure rate was found to be statistically lower than the 809 nm and 1070 nm closure rates (* *) ($p<0.05$). On day 4, the CI of the sutured incisions was statistically less than that of the laser-irradiated groups (* *) ($p<0.05$)

4.4.5 Thermally altered areas

Different thermal effects: hyperthermia and coagulation, were observed on the laser-irradiated skin tissue. The thermal damage around the welded area was monitored during the recovery period and quantified (Figure 4.22). On day 1, thermal damage was greater in the 809 nm and 980 nm laser groups than in the 1070 nm YFL-irradiated group ($p<0.05$). On day 4, follow up showed a 50% recovery of hyperthermia tissue irradiated with 1070 nm laser. That zone remained the same in the 809 nm-irradiated tissue and decreased to one-third in the 980 nm-irradiated tissue from day 1 to day 4.

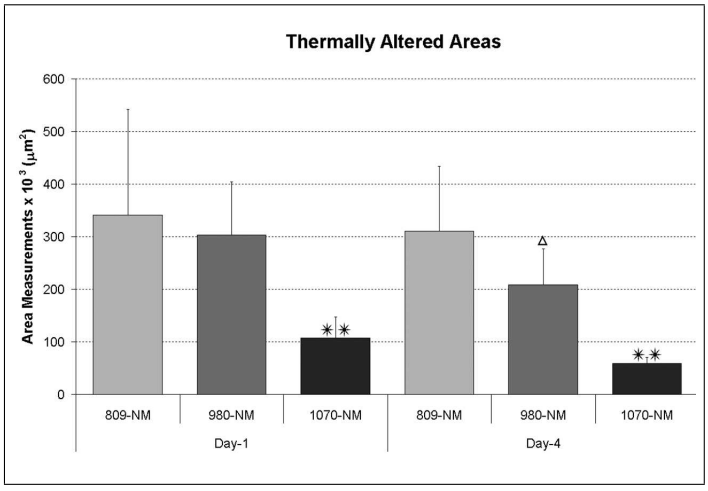

Figure 4.22 Different near infrared laser irradiation at the same energy level (79.61 J/cm^2) resulting in different extents of thermal zones. The thermal hazard of 1070 nm laser welding was minimum on day 1 and on day 4 ($p<0.05$). On the 4th postoperative day, the thermal zones of the 980 nm laser-irradiated incisions were statistically smaller than those of the 809 nm irradiated incisions (Δ) ($p<0.05$). Soldering (ICG+BSA) with the 809 nm diode laser was the most thermally hazardous of all the lasers on day 4 ($p<0.05$). No tissue carbonization was observed in any of the applications

4.4.6 Granulation tissue area

Granulation tissue had started to form on the 4th postoperative day only in the 809 nm and 1070 nm irradiated samples. On day 7; only the GAs of the 809 nm soldered incisions were found to be significantly greater, on average, than those in the suture group ($p<0.05$). On day 14, granulation areas of both 809 nm and 1070 nm laser groups were found to be significantly greater than those of the suture group. Moreover, the granulation response of the 980 nm group was found to be significantly

less than that of the 1070 nm and 809 nm groups. Granulation tissue measurement on day 21 showed no statistical difference between experimental groups (Figure 4.23).

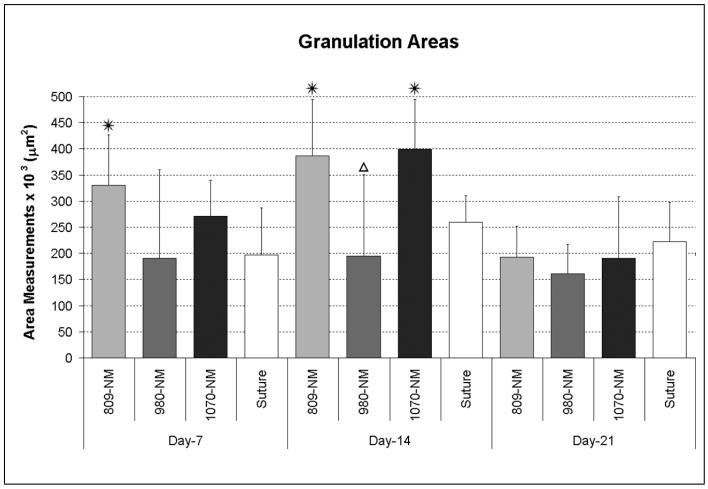

Figure 4.23 Granulation area (GA) measurements. 809-nm granulation was statistically higher ($p<0.05$) than the control group on Day-7 and on Day-14. On Day-14, 1070-nm irradiated samples GA were statistically higher than the control group ($p<0.05$). There were no significant difference between 980-nm welded group and control group throughout the recovery period. Moreover, 980-nm welded incisions GA was statistically smaller than 1070-nm and 809-nm welded incisions GA (Δ). On Day-21, no statistical difference among experimental groups was found.

4.4.7 Epidermal thickness

One of the indicators of wound healing is the change in epidermal thickness (ET). It normally starts at a higher value and gradually decreases to a certain level, depending on the degree of the trauma. In our study the normal value of the epidermal thickness was approximately 30-40 μm. Measurements were reported from day 4 (not applicable for day 1). For the suture (control) group, epidermal thickness decreased gradually, from 110 μm (day 4) to 40 μm (day 21). This was taken as the normal response of the tissue. The 809 nm and 980 nm laser-irradiated incisions reached their maximum ETs on day 7: 106.4 μm and 134.8 μm, respectively, as well as the maximum ETs among the other experimental groups throughout the follow-up period. On day 14, the average epidermal thicknesses of the 809 nm and 980 nm groups decreased to the suture (control) group levels. On day 21, the epidermal thicknesses of all groups' incisions showed no statistical difference and were around the 35-40 μm level ($p<0.05$). The most impressive results for epidermal thickness were obtained from the 1070 nm laser

irradiated samples: there was almost no thickening (≈35 μm) following the operation and during the 21-day recovery period (Figure 4.24).

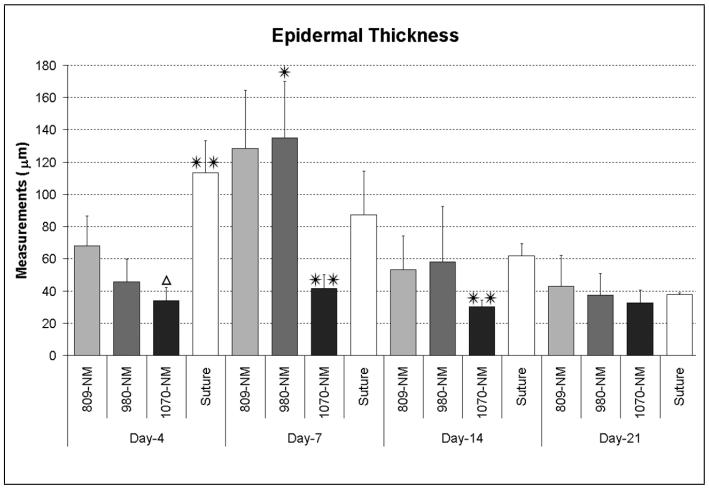

Figure 4.24 Epidermal thickness (ET) measurements. On day 4, control group epidermal thickness was statistically greater than that of the laser-irradiated groups. The ET of the 1,070 nm-welded incisions was statistically significantly thicker than that of the 809 nm soldered incisions (Δ) ($p<0.05$). On day 7, the ET of the 980 nm welded incisions was greater than that of the control group (*) ($p<0.05$). On both day 7 and day 14, the ET of the 1070 nm welded incisions was minimal (* *)

4.4.8 Mechanical Examinations: Tensile Tests

Tensile strengths for all groups are shown in Figure 4.25. Measurement was not applicable for sutured incisions on day 1 (the incisions had not closed). On day 1, the tensile strength of the 809 nm group was found to be weakest within the laser groups ($p<0.05$). However, its value was as great as the strength of the sutured group on day 7. This situation was much more striking for the 980 nm and 1070 nm groups: the welded incisions on day 1 were found to be stronger than those of the sutured group on day 7. The welding abilities of the 980 nm and 1070 nm lasers were still noticeable on day 4: tensile strength was greater than that of the 809 nm-soldered and sutured incisions ($p<0.05$). There was no difference between 809 nm and sutured groups. On day 7, 980 nm-welded incisions had the greatest tensile strength ($p<0.05$) compared with the other groups. Tensile strengths of the 809 nm-soldered and 1,070 nm welded incisions were also found to be greater than those of the sutured incisions ($p<0.05$). On day 14, the tensile strengths of all the groups had almost the same values, except for the 809 nm laser-soldering group. It was significantly greater than that of the suture

(control) group and the 1070 nm laser-welding group. On day 21, the tensile strengths of the laser-welded incisions (980 nm and 1070 nm) were greater than that of the suture (control) group ($p<0.05$). Although 809 nm-soldered incisions seemed to be stronger than sutured incisions, there was no statistically significant difference ($p=0.09$).

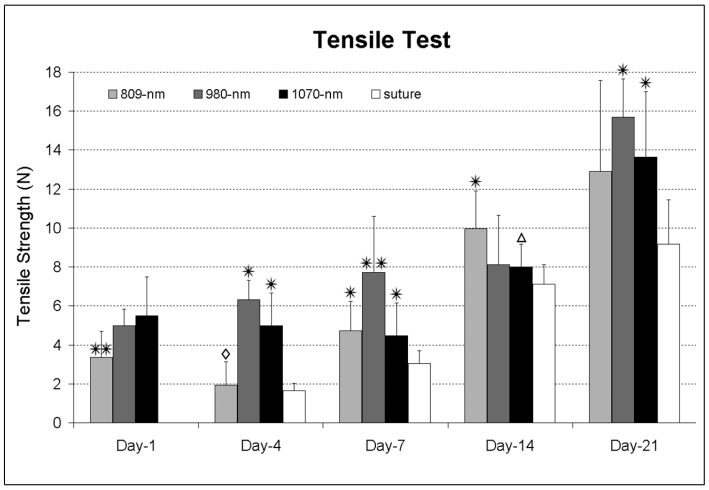

Figure 4.25 Mechanical (tensile) test results. On day 1, the tensile strengths of the 809 nm closed incisions were weaker than those of the welded incisions (**) ($p<0.05$). On day 4, the tensile strengths of the 980 nm and 1070 nm welded incisions were greater than those of the 809 nm soldered (◇) and the sutured (*) incisions. On day 7, the 980 nm-welded incisions had maximum tensile strength (**) ($p<0.05$). Tensile strength of the 809 nm-soldered and 1,070 nm welded incisions were great than those of the sutured incisions (*) ($p<0.05$). On day 14, there was a significant difference in tensile strengths between the 809 nm-soldered and 1070 nm-welded (Δ) incisions, as well as the control group and soldered group (*). On day 21, tensile strengths of the laser-welded incisions (980 nm and 1070 nm) were greater than in the control group (*) ($p<0.05$)

4.5 Discussion

Macro-inspection of the 21-day wound recovery period revealed data about the possible abnormalities around the incision site, such as infection and thermal damage. Incisions and parts closed due to recovery and welding were measured and quantified in terms of closure index. Thermally altered areas were also measured under microscopic examination; granulation area and epidermal thickness were considered as semi-quantitative indicators of wound healing of sutured wounds and laser welds. Thermal damage or any infectious hazard was covered by newly formed granulation tissue. Thermal and morphological alterations of skin tissue change the micro-structures (collagen linearity or crosswise pattern, coagulation hardened structure) and eventually

lead to change in the mechanical properties. Therefore, the strength of the incisions was compared in terms of tensile test results. The sutured group as the control was examined on a daily basis, and no serious abnormalities were recorded. On day 1 and day 4, although there was no sign of infection, needle holes, and openings on the sutured incisions still remained as possible entrance points for microbial pathogens. Even though the suture material itself had been pronounced as a potential source of infection, we did not record any cases supporting that hypothesis [110]. Although there was no sign of infection, the healed incision was not found to be regularly shaped, as was observed in the welded cases. A deep incision line and vertically oriented suture marks were visible until the end of the 21 days of recovery in the suture group. Visibility of the scar was minimal in the 1070 nm group, while, for the other laser groups, because of thermal effect, the scar was more or less evident.

Thermal effects are the weakest parts of laser welding and can directly determine the physical appearance and recovery period of the welded wound [111]. For the 809 nm laser soldering group, photothermal interactions resulted in the carbonization of the solder mixture (ICG + BSA) accumulated on the top of the incision. A rapid increase in temperature due to high heat deposition caused some serum albumin to become carbonized just in between the lips of the incisions. Solder mixture was used to absorb the 809 nm wavelength energy selectively at the incision site, but laser light was not totally absorbed at that layer and was propagated deeper into the sites. This was clearly seen through microscopic examination. Therefore, temperature increase was not limited by the solder and could be traced down to the deeper layers. Moreover, vaporization of tissue water pushed the solder mixture (placed in between the lips of the incision) to the surface, and, hence, scar formation was irregular in shape. Even though 809 nm laser soldering enhanced immediate closure, depending on the severe thermal effect, skin tissue responded with a high level of granulation around the incision and the formation of a relatively thicker epidermis in the early phases of recovery. Additionally, this technique was found to be mechanically the weakest one when compared with other lasers, but it was still better than suturing. Cooper et al. examined tissue soldering with varying ICG concentrations and 810 nm laser power densities; a power density of 15.9 W/cm^2, the same as power density on skin tissue in this study, and the ICG doped

albumin solder (ICG 2.5 mg/ml) provided the most controlled delivery to target tissue within an average of 12.1 s, and, at a power density of 15.9 W/cm^2 or below, increasing ICG concentrations did appear to result in significant increases in tensile strengths [87]. Kirsch et al. reported that superior immediate tensile strength was obtained with a diode laser and ICG/albumin solder at a power density of 31.8 W/cm^2, and it was equivalent to the tensile strength of a 7-day healed sutured wound [112]. In another comparative study by Kirsch and colleagues, an 810 nm laser (16 W/cm^2) was applied to rat skin in combination with albumin and ICG [88]. The tensile strengths of laser-soldered samples were significantly stronger on both the 7th and 10th post-operative days than those of sutured wounds. The results of our study were in accordance with those cited above: the day 1 tensile strength of the 809 nm soldering group was equivalent to the strength of the day 7 suture group; moreover, the other lasers (980 nm and 1070 nm) were found to produce greater strengths than the 809 nm soldering group.

Macro-inspection throughout the 21-day recovery period showed that the 980 nm laser group also had the disadvantage of thermal side effects, at least during the early phase (days 1 and 4). The 980 nm wavelength laser, which was relatively absorbed on the upper layers of the dermis mostly by water molecules, resulted in sealing of the incisions. Carbonization of blood leakage from inner parts of the incision was also observed in the early phase of recovery. The overall photothermal effect of this wavelength was as severe as that of 809 nm on day 1, but recovery was faster, and, on day 4, the effect was found to be significantly less than at 809 nm. Thus, it did not increase granulation above normal levels (with reference to the control group). However, carbonization of blood delayed the normal development of the epidermis; it took 14 days for the epidermal thickness to decrease to normal values. The superficial closing ability of the 980 nm laser in the early phases of recovery was almost the same as with the other lasers, and mechanical tests showed that, just after 1 week, the welds became as strong as the sutures after a 21-day recovery. At the end of the 21-day recovery period, tensile strength in the 980 nm group was found to be almost two-times greater than that of the control group. Macro and micro examination showed that the 1070 nm-welded incisions had the maximal apposition with least thermal

damage. Immediate closure ability was similar to that of the other lasers; however, the thermal effect was almost invisible on the macroscopic scale. Epidermal thickening was noted to be stationary in the range of normal values during all the recovery period. In addition, the mechanical strength of the 1070 nm welds was found to be better than that of the conventional sutures throughout the recovery period and as strong as those of the other lasers at the end of the 21-day recovery period. Fried et al. reported that 1064 nm laser welds with India ink showed less thermally induced tissue damage than reported in previous skin welding studies [52]. In this study we found that the 1070 nm fiber laser gave a better performance (minimal thermal damage and better tensile strength than that of the control and other laser groups) without the application of any chromophores. No stay sutures, biological adhesives or chemical agents were used, and the incisions healed without dehiscence and abnormal scarring.

According to the results obtained, laser welding was found to be reliable in terms of immediate and mechanically strong closure in comparison with suturing. Laser welding is a photothermal process, and thermal damage to the surrounding tissue can be observed. The extent of photothermal effects can be minimized with the selection of a suitable laser wavelength and the correct dose. Soldering with the 809 nm laser was found to be capable of creating strong full-thickness closure, but thermal damage was evident, both on the macroscopic and microscopic scale. The thermal damage from 980 nm laser welding was found to be more tolerable, and it could create one-third-thick welds just at the beginning of the healing period (on day 1), with a tensile strength better than that found in the sutured incisions after 7 days of healing. Thus, it would be better to use 980 nm laser for welding incisions on skin tissue wrapping around joints or moving organs by providing immediate and robust closure. The results showed that 1070 nm laser welding produced noticeably stronger bonds with minimal scar formation; thus, it could be preferred for plastic surgery for cosmetic reasons.

5. CONCLUSION

This study is a comprehensive comparative research which has accomplished the following tasks:

1- Comparison of laser welding and suturing methods on a surgical skin incision

Two closure methodologies served a physical approximation for edges of incision. Laser energy went one step further and managed to seal the gap leakproof. No redness which is a sign of pus formation was observed macroscopically in any of the incision closed with either lasers. Tensile strength gained at the end of the first week of healing period for suture closed incisions had been already achieved in 24 hours post surgery by laser welding. At the end of 21-Days follow up of recovery period, tensile strengths of laser-welded incisions were greater than in the control group. This shows that laser welding is advantageous over suturing.

2- Comparison of effects of different wavelengths on skin tissue welding

Three near infrared wavelengths (809, 980 and 1070 nm) were compared and found to have different welding abilities. Each of these wavelengths should be chosen for specific welding purpose. For instance, any incision on face can be closed by 1070 nm laser for aesthetic appearance whereas strong closure in skin tissue over joints can be obtained by 980 nm laser application.

3- Comparison of effects of different irradiance levels on skin tissue at 980 nm

Although almost the same energy ($\approx 2.4 - 2.5$ J) of a wavelength was delivered to the tissue, different power and application time combinations brought about different consequences on skin tissue welding. It was shown that thermal hazard causes delay in recovery of tensile strength although high closure rates through dermal layer was

obtained with such an application.

4- Establishment of experimental protocols and measurement techniques

All surgical operations, histological and mechanical tests were performed by the author. Full-thickness incisions were done through skin tissue. Laser applications were done precisely spot by spot having cooling time intervals in between. Changes in tissue structure were observed by general staining method combined with special microscopy techniques. Macroscopic and microscopic inspections were quantified, resulting in new terminology for future studies: Closure Index, Thermally Altered Area, Granulation Area, and Epidermal Thickness. All the mentioned inspections were performed on particular days at given period of surgical incision healing. Progress of bonding was measured as tensile strength through the same particular days, thus histological findings were evaluated from mechanical point of view or vice versa.

To appreciate temperature of the surface of the heated cut is important in order not to give thermal damage to the surrounding tissue. The rate of heat generation [W/m^3] as a function of depth depends upon the optical penetration depth of the laser beam. The resulting temperature profiles are governed by heat conduction in the tissue and thickness of the tissue relative to the optical penetration depth and thermal boundary conditions. Thermal denaturation of tissue proteins has been known as a rate process related to the local temperature-time response. Control of tissue surface temperature within a narrow margin can eliminate rapidly increasing temperatures.

Accumulated damage Ω increases at a constant rate when tissue temperature is held constant (Figure 5.1). Yet for linearly increasing temperature, the rate of increase in accumulated damage is exponential, suggesting an accelerated rate of thermal damage to tissue that can appear in milliseconds.

Radiometric methods in combination with computer-assisted temperature feedback control have been used to maintain tissue surface temperature at some desired value. Using such control reduced the danger of overheating and prevented thermal

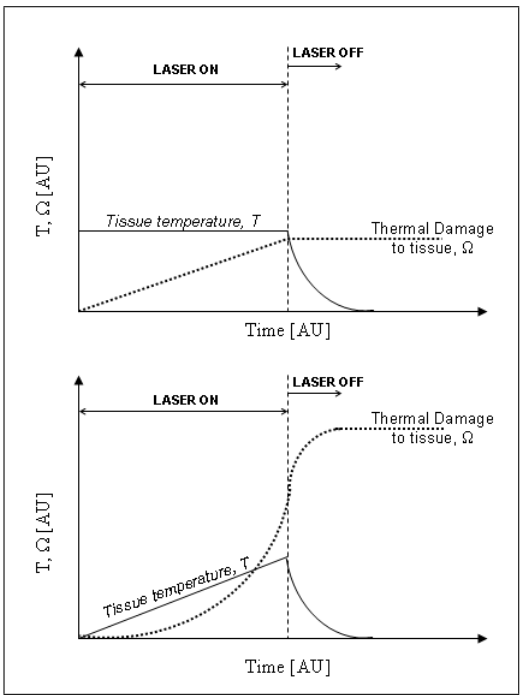

Figure 5.1 Rate process model of thermal damage to tissue as a function of tissue temperature during and after laser irradiation: (top) constant tissue temperature while laser is on, and (bottom) sudden increase in temperature during laser irradiation [62].

injury to the tissue. In this thesis work no radiometric temperature measurement was tried for surface temperature change during laser irradiations. This was the missing part of experiments and will be performed for future studies. Instead, change in temperature under dermal layer was tried to be detected by K-type thermocouple during laser irradiation. Such systems should respond quick enough to detect instant (1-5 ms) changes. Our system respond time was 250 ms and gave averages of 8 measurements in every 2 seconds. In this respect, measurements cannot be regarded as reliable.

The study showed that near infrared lasers are important candidates for skin tissue welding in clinical and surgical applications. Depending on the aim of the application, different laser wavelengths can be chosen. In future work, different modes of operation could be tested; laser energy could be delivered in modulated fashion. In addition, more than one wavelength (1070 nm for deep welding and 980 nm for superficial use) could be applied for more efficient welding with thermal monitoring systems.

REFERENCES

1. Yahr, W. Z., and K. J. Strully, "Non-occlusive small arterial anastomosis with neodymium laser," *Surg Forum*, Vol. 15, p. 224, 1964.

2. McNally-Heintzelman, K. M., and A. J. Welch, "Laser tissue welding," in *Biomedical Photonics Handbook* (Tuan, V. D., ed.), ch. 39, pp. 39(1)–39(45), New York: CRC Press LLC, 2nd edition ed., 2003.

3. Schober, R., F. Ulrich, T. Sander, H. Durselen, and S. Hessel, "Laser-induced alteration of collagen substructure allows microsurgical tissue welding," *Science*, Vol. 232, pp. 1421–1422, 1986.

4. Tang, J., G. Godlewski, S. Rouy, and G. Delacretaz, "Morphologic changes in collagen fibers after 830 nm diode laser welding," *Lasers Surg Med*, Vol. 21, no. 4, pp. 438–443, 1997.

5. Bass, L. S., N. Moazami, and J. Pocsidio, "Changes in Type-I collagen following laser welding," *Lasers Surg Med*, Vol. 12, pp. 500–505, 1992.

6. Vale, B. H., A. Frenkel, and S. Trenka-Benthin, "Microsurgical anastomosis of rat carotid arteries with the CO_2 laser," *Plast Reconstr Surg*, Vol. 77, pp. 759–766, 1986.

7. Menovsky, T., J. F. Beek, and M. J. C. van Gemert, "Laser tissue welding of dura mater and peripheral nerves: A scanning electron microscopy study," *Lasers Surg Med*, Vol. 19, pp. 152–158, 1996.

8. Godlewski, G., S. Rouy, and M. Dauzat, "Ultrastructural study of arterial wall repair after argon laser microanastomosis," *Lasers Surg Med*, Vol. 7, pp. 258–262, 1987.

9. A, W. R., G. E. Kopchock, and C. E. Donayre, "Mechanism of tissue fusion in argon laser-welded vein artery anastomoses," *Lasers Surg Med*, pp. 83–89, 1988.

10. Kada, O., K. Shimizu, and H. Ikuta, "An alternative method of vascular anastomosis by laser: Experimental and clinical study," *Lasers Surg Med*, Vol. 7, pp. 240–248, 1987.

11. Constantinescu, M. A., A. Alfieri, G. Mihalache, F. Stuker, A. Ducray, R. W. Seiler, and M. F. . M. Reinert, "Effect of laser soldering irradiation on covalent bonds of pure collagen," *Lasers Med Sci*, Vol. 22, pp. 10–14, 2007.

12. Mustoe, T. A., G. F. Pierce, A. Thomason, P. Gramates, M. B. Sporn, and T. F. Deuel, "Accelerated healing of incisional wounds in rats induced by transforming growth factor-β," *Science*, Vol. 237, no. 4820, pp. 1333–1336, 1987.

13. Stadelmann, W. K., A. G. Digenis, and G. R. Tobin, "Physiology and healing dynamics of chronic cutaneous wounds," *Am J Surg (Suppl 2A)*, Vol. 176, pp. 26S–38S, 1998.

14. Ross, R., and E. P. Benditt, "Wound healing and collagen formation: Fine structure in experimental scurvy," *J Cell Biol*, Vol. 12, pp. 533–551, 1962.

15. Williamson, D., and K. Harding, "Wound healing," *Medicine*, Vol. 32, no. 12, pp. 4–7, 2004.

16. Lindstedt, E., and P. Sandblom, "Wound healing in man: Tensile strength of healing wounds in some patient groups," *Ann Surg*, Vol. 181, no. 6, pp. 842–846, 1975.

17. Ordman, L. J., and T. Gillman, "Studies in the healing of cutaneous wounds," *Arch Surg*, Vol. 93, no. 6, pp. 857–882, 1966.

18. Prockop, D., "What holds us together? Why do some of us fail apart? What can we do about it?," *Matrix Biology*, Vol. 16, pp. 519–528, 1998.

19. Hochberg, J., K. M. Meyer, and M. D. Marion, "Suture choice and other methods of skin closure," *Surg Clin N Am*, Vol. 89, pp. 627–641, 2009.

20. Quinn, J., J. Maw, K. Ramotar, G. Wenckebach, and G. Wells, "Octylcyanoacrylate tissue adhesive versus suture wound repair in a contaminated wound model," *J Vasc Surg*, Vol. 122, no. 1, pp. 69–72, 1997.

21. Quinn, J., G. Wells, T. Sutcliffe, M. Jarmuske, J. Maw, I. Stiell, and P. Johns, "Tissue adhesive versus suture wound repair at 1 year: Randomized clinical trial correlating early, 3-month, and 1-year cosmetic outcome," *Annals of Emergency Medicine*, Vol. 32, no. 6, pp. 645–649, 1998.

22. Leaper, D. J., A. V. Pollock, and M. Evans, "Abdominal wound closure: A trial of nylon, polyglycolic acid and steel sutures," *British Journal of Surgery*, Vol. 64, no. 8, pp. 603–606, 2005.

23. Barnett, P., F. C. Jarman, J. Goodge, G. Silk, and R. Aickin, "Randomised trial of histoacryl blue tissue adhesive glue versus suturing in the repair of paediatric lacerations," *J. Paediatr. Child Health*, Vol. 34, no. 8, pp. 548–550, 1998.

24. Hollander, J. E., and A. J. Singer, "Application of tissue adhesives: Rapid attainment of proficiency," *Academic Emergency Medicine*, Vol. 5, no. 10, pp. 1012–1017, 1998.

25. Agarwal, A., D. Kumar, S. Jacob, C. Baid, A. Agarwal, and S. Srinivasan, "Fibrin glue assisted sutureless posterior chamber intraocular lens implantation in eyes with deficient posterior capsules," *J Cat Ref Surg*, Vol. 34, no. 9, pp. 1433–1438, 2008.

26. Babetty, Z., A. Sumer, and S. Altintas, "Knot properties of alternating sliding knots with different patterns in comparison to alternating and simple sliding knots," *J Am Coll Surg*, Vol. 186, no. 5, pp. 485–489, 1998.

27. Babetty, Z., A. Sumer, S. Altintas, S. Erguney, and S. Goksel, "Changes in knot holding capacity of sliding knots in vivo and tissue reaction," *Arch Surg*, Vol. 133, pp. 727–734, 1998.

28. Altman, G. H., F. Diaz, C. Jakuba, T. Calabro, R. L. Horan, J. Chen, H. Lu, J. Richmond, and D. L. Kaplan, "Silk based biomaterials," *Biomaterials*, Vol. 24, no. 3, pp. 401–416, 2003.

29. Parell, G. J., and G. D. Becker, "Comparison of absorbable with nonabsorbable sutures in closure of facial skin wounds," *Arch Facial Plast Surg*, Vol. 5, pp. 488–490, 2003.

30. Austin, P. E., K. A. Dunn, K. E. Cofield, C. K. Brown, W. A. Wooden, and J. F. Bradfield, "Subcuticular sutures and the rate of inflammation in noncontaminated wounds," *Ann Emerg Med*, Vol. 25, no. 3, pp. 328–330, 1995.

31. Moy, R. L., B. Waldman, and D. W. Hein, "A review of sutures and suturing techniques," *J Dermatol Surg Oncol*, Vol. 18, pp. 785–795, 1992.

32. Bass, L., and M. Treat, "Laser tissue welding: A comprehensive review of current and future clinical applications," *Lasers Surg Med*, Vol. 17, pp. 315–349, 1995.

33. Barrerias, D., P. P. Reddy, G. A. McLorie, D. Bagli, A. E. Khoury, W. Farhat, L. Lilge, and P. A. Merguerian, "Lessons learned from laser tissue soldering and fibrin glue pyeloplasty in an in vivo porcine model," *J Urol*, Vol. 164, no. 3, p. 1106, 2000.

34. Wolf, J. S., J. J. Soble, S. Y. Nakada, H. J. Rayala, P. A. Humphrey, R. V. Clayman, and D. P. Poppas, "Comparison of fibrin glue, laser weld, and mecanical suturing device for laparoscopic closure of ureterotomy in a porcine model," *J Urol*, Vol. 157, no. 4, p. 1487, 1997.

35. Zhang, L., A. R. Kolker, E. I. Choe, N. Bakshandeh, G. Josephson, F. C. Wu, J. W. Sieberrt, and A. K. Kasabian, "Venous microanastomosis with unilink system, sleeve, and suture techniques: A comparative study in the rat," *J Reconst Microsurg*, Vol. 13, no. 4, p. 257, 1997.

36. Pursifull, N. F., and A. F. Morey, "Tissue glues and nonsuturing techniques," *Current Opinion in Urology*, Vol. 17, no. 6, pp. 396–401, 2007.

37. Durham, L. H., D. J. Willatt, M. W. Yung, I. Jones, P. A. Stevenson, and M. F. Ramadan, "A method for preparation of fibrin glue," *J Laryn Otol (1987), 101:1182-1186*, Vol. 101, pp. 1182–1186, 1987.

38. Godlewski, G., S. Rouy, J. Tang, M. Dauzat, F. Chambettaz, and R. P. Salathe, "Scanning electron microscopy of microarterial anastomoses with a diode laser: Comparison with conventional manual suture," *J Reconstr Microsurg*, Vol. 11, no. 1, pp. 33–40, 1995.

39. Hasegawa, M., T. Sakurai, M. Matsushita, N. Nishikimi, Y. Nimura, and M. Kobayashi, "Comparison of argon-laser welded and sutured repair of inferior vena cava in canine model," *Lasers Surg Med*, Vol. 29, no. 1, pp. 60–68, 2001.

40. Capon, A., E. Souil, B. Gauthier, C. Sumian, M. Bachelet, B. Buys, B. S. Polla, and S. Mordon, "Laser assisted skin closure (LASC) by using a 815-nm diode-laser system accelerates and improves wound healing," *Lasers Surg Med*, Vol. 28, pp. 168–175, 2001.

41. Chikamatsu, E., T. Sakurai, N. Nishikimi, T. Yano, and Y. Nimura, "Comparison of laser vascular welding, interrupted stures, and continuous sutures in growing vascular anastomoses," *Lasers Surg Med*, Vol. 16, no. 1, pp. 32–41, 1995.

42. Çilesiz, I. F., *Thermal Feedback Control During Laser-Assisted Tissue Welding*. PhD thesis, The University of Texas at Austin, Texas, USA, 1994.

43. McNally, K. M., J. M. Dawes, A. E. Parker, A. Lauto, J. A. Piper, and E. R. Owen, "Laser-activated solid protein solder for nerve repair: In vitro studies of tensile strength and solder/tissue temperature," *Lasers Med Sci*, Vol. 14, pp. 228–237, 1999.

44. Welch, A. J., J. H. Torres, and W. F. Cheong, "Laser physics and laser-tissue interaction," *Texas Heart Inst J*, Vol. 16, pp. 141–149, 1989.

45. Welch, A. J., M. J. C. van Gemert, W. Star, and B. Wilson, *Optical-Thermal Response of Laser-Irradiated Tissue*, New York: Plenum Press, 1st edition ed., 1995.

46. Welch, A. J., "The thermal response of laser irradiated tissue," *IEEE J Quantum Electron*, Vol. QE-20, no. 12, pp. 1471–1481, 1984.

47. Chen, B., S. L. Thomsen, R. J. Thomas, J. Oliver, and A. J. Welch, "Histological and modeling study of skin thermal injury to 2.0 μm laser irradiation," *Laser Surg Med*, Vol. 40, pp. 358–370, 2008.

48. Springer, T. A., and A. J. Welch, "Temperature control during laser vessel welding," *Appl Opt*, Vol. 32, no. 4, pp. 517–525, 1993.

49. Oz, M. C., L. S. Bass, H. W. Popp, R. S. Chuck, J. P. Johnson, S. L. Trokel, and M. R. Treat, "In vitro comparison of thulium-holmium-chromium:YAG and argon ion lasers for welding biliary tissue," *Lasers Surg Med*, Vol. 9, no. 3, pp. 245–252, 1989.

50. Menovsky, T., J. F. Beek, and M. J. C. van Gemert, "CO_2 laser nerve welding: Optimal laser parameters and the use of solders in vitro," *Microsurgery*, Vol. 15, no. 1, pp. 44–49, 1994.

51. Brooks, S. G., S. Ashley, J. Fisher, G. A. Davies, J. Griffiths, R. C. Kester, and M. R. Rees, "Exogenous chromophores for the argon and Nd:YAG lasers: A potential application to laser-tissue interactions," *Lasers Surg Med*, Vol. 12, pp. 294–301, 1992.

52. Fried, N. M., and T. Walsh, "Laser skin welding: In vivo tensile strength and wound healing results," *Lasers Surg Med*, Vol. 27, no. 1, pp. 55–63, 2000.

53. "Optical constants of ice from the ultraviolet to the microwave," *http://omlc.ogi.edu/spectra/water/data/warren95.dat*.

54. Walsh, J. T., T. J. Flotte, and T. F. Deutsch, "Er:YAG laser ablation of tissue: Effect of pulse duration and tissue type on thermal damage," *Lasers Surg Med*, Vol. 9, pp. 314–326, 1989.

55. van Gemert, M. J. C., and A. J. Welch, "Clinical use of laser-tissue interactions," *IEEE Eng Med Biol Mag*, Vol. December, pp. 10–13, 1989.

56. Simhon, D., A. Ravid, M. Halpern, I. Çilesiz, T. Brosh, N. Kariv, A. Leviav, and A. Katzir, "Laser soldering of rat skin, using fiberoptic temperature controlled system," *Lasers Surg Med*, Vol. 29, no. 2, pp. 265–273, 2001.

57. Eyal, O., and A. Katzir, "Thermal feedback control techniques for transistor-transistor logic triggered CO_2 laser used for irradiation of biological tissue utilizing infrared fiberoptic radiometry," *Appl Opt*, Vol. 33, no. 9, pp. 1751–1754, 1994.

58. Simhon, D., T. Brosh, M. Halpern, A. Ravid, T. Vasilyev, N. Kariv, A. Katzir, and Z. Nevo, "Closure of skin incisions in rabbits by laser soldering I: Wound healing pattern," *Lasers Surg Med*, Vol. 35, pp. 1–11, 2004.

59. Brosh, T., D. Simhon, M. Halpern, A. Ravid, T. Vasilyev, N. Kariv, Z. Nevo, and A. Katzir, "Closure of skin incisions in rabbits by laser soldering-II: Tensile strength," *Lasers Surg Med*, Vol. 35, pp. 12–17, 2004.

60. Simhon, D., M. Halpern, T. Brosh, T. Vasilyev, A. Ravid, T. Tennenbaum, Z. Nevo, and A. Katzir, "Immediate tight sealing of skin incisions using an innovative temperature-controlled laser soldering device in vivo study in porcine skin," *Anals of Surgery*, Vol. 245, no. 2, pp. 206–213, 2007.

61. Lobel, B., O. Eyal, N. Kariv, and A. Katzir, "Temperature controlled CO_2 laser welding of soft tissues: Urinary bladder welding in different animal models (rats, rabbits, and cats)," *Lasers Surg Med*, Vol. 26, pp. 4–12, 2000.

62. Çilesiz, I., S. Thomsen, and A. J. Welch, "Controlled temperature tissue fusion: Argon laser welding of rat intestine in vivo, Part one," *Lasers Surg Med*, Vol. 21, pp. 269–277, 1997.

63. Çilesiz, I., S. Thomsen, A. J. Welch, and E. K. Chan, "Controlled temperature tissue fusion: Ho:YAG laser welding of rat intestine in vivo, Part two," *Lasers Surg Med*, Vol. 21, pp. 278–286, 1997.

64. Spector, D., Y. Rabi, I. Vasserman, A. Hardy, J. Klausner, M. Rabau, and A. Katzir, "In vitro large diameter bowel anastomosis using a temperature controlled laser tissue soldering system and albumin stent," *Lasers Surg Med*, Vol. 41, pp. 504–508, 2009.

65. Lauto, A., R. Trickett, R. Malik, J. Dawes, and E. Owen, "Laser activated solid protein bands for peripheral nerve repair: An in vivo study," *Laser Surg Med*, Vol. 21, pp. 134–141, 1997.

66. Hodges, D. E., K. M. McNally, and A. J. Welch, "Surgical adhesives for laser-assisted wound closure," *Journal of Biomedical Optics*, Vol. 6, no. 4, pp. 427–431, 2001.

67. Chivers, R. A., "In vitro tissue welding using albumin solder: bond strengths and bonding temperatures," *Int J Adhesion Adhesives*, Vol. 20, pp. 179–187, 2000.

68. Fujita, M., Y. Morimoto, S. Ohmori, N. Usami, T. Arai, T. Maehara, and M. Kikuchi, "Preliminary study of laser welding for aortic dissection in a porcine model using a diode laser with indocyanine green," *Lasers Surg Med*, Vol. 32, pp. 341–345, 2003.

69. Birch, J. F., D. J. Mandley, S. L. Williams, D. R. Worrall, P. J. Trotter, F. Wilkinson, and P. R. Bell, "Methylene blue based protein solder for vascular anastomoses: An in vitro burst pressure study," *Lasers Surg Med*, Vol. 23, pp. 323–329, 2000.

70. Oz, M. C., S. Prangi, R. S. Chuck, C. C. Marboe, L. S. Bass, R. Nowygrod, and M. R. Treat, "Tissue soldering by use of indocyanine green dye-enhanced fibrinogen with the near infrared diode laser," *J Vasc Surg*, Vol. 5, pp. 718–725, 1990.

71. McNally, K. M., B. S. Sorg, E. K. Chan, A. J. Welch, J. M. Dawes, and E. R. Owen, "Optimal parameters for laser tissue soldering. Part-I: Tensile strength and scanning electron microscopy analysis," *Lasers Surg Med*, Vol. 24, pp. 319–331, 1999.

72. McNally, K. M., B. S. Sorg, and A. J. Welch, "Novel solid protein solder designs for laser-assisted tissue repair," *Lasers Surg Med*, Vol. 27, pp. 147–157, 2000.

73. Lauto, A., M. Stoodley, A. Avolio, M. Sarris, G. McKenzie, D. D. Sampson, and L. J. R. Foster, "In vitro and in vivo tissue repair with laser-activated chitosan adhesive," *Laser Surg Med*, Vol. 39, pp. 19–27, 2007.

74. Ishihara, M., K. Nakanishi, K. Ono, M. Sato, M. Kikuci, Y. Saito, H. Yura, T. Matsui, H. Hattori, M. Uenoyama, and A. Kurita, "Photocrosslinkable chitosan as a dressing for wound occlusion and accelerator in healing process," *Biomaterials*, Vol. 23, pp. 833–840, 2002.

75. Lauto, A., D. Mawad, and L. J. R. Foster, "Review adhesive biomaterials for tissue reconstruction," *J Chem Technol Biotechnol*, Vol. 83, pp. 464–472, 2008.

76. Geldi, C., "Microcontroller based high power 809-nm diode laser design for photodynamic therapy (PDT) applications," Master's thesis, Boğaziçi University, Istanbul, Turkey, 2003.

77. Geldi, C., O. Bozkulak, H. O. Tabakoglu, S. Isci, A. Kurt, and M. Gulsoy, "Development of a surgical diode-laser system: Controlling the mode of operation," *Photomed and Laser Surg*, Vol. 24, no. 6, pp. 733–739, 2006.

78. Geldi, C., O. Bozkulak, H. O. Tabakoglu, S. Isci, O. Kalkanci, A. Kurt, and M. Gulsoy, "Microcontroller based surgical diode laser system," pp. 44–47, 2004.

79. Lauto, A., R. Stewart, M. Ohebshalom, N. D. Nikkoi, D. Felsen, and D. P. Poppas, "Impact of solubility on laser tissue-welding with albumin solid solders," *Lasers Surg Med*, Vol. 28, no. 1, pp. 44–49, 2001.

80. Bass, L. S., S. K. Libutti, and A. M. Eaton, "New solders for laser welding and sealing," *Lasers Surg Med Supplement*, Vol. 5, no. 2, p. 63, 1993.

81. Sauda, K., T. Imasaka, and N. Ishibashi, "Determination of protein in human serum by high performance liquid chromatography," *Anal Chem*, Vol. 58, pp. 2649–2653, 1986.

82. Moazami, N., M. C. Oz, L. S. Bass, and M. R. Treat, "Reinforcement of colonic anastomoses with laser and dye-enhanced fibrinogen," *Arch Surg*, Vol. 125, pp. 1452–1454, 1990.

83. Oz, M. C., S. K. Libutti, R. C. Ashton, J. F. Lontz, G. M. Lemole, and R. Nowygrod, "Comparison of laser-assisted fibrinogenbonded and sutured canine arteriovenous anastomoses," *Surgery*, Vol. 112, pp. 76–83, 1992.

84. Kirsch, A. J., G. E. Dean, M. C. Oz, S. K. Libutti, M. R. Treat, R. Nowygrod, and T. W. Hensle, "Preliminary results of laser tissue welding in extravesical reimplantation of the ureters," *J Urol*, Vol. 151, pp. 514–517, 1994.

85. Kirsch, A. J., M. I. Miller, T. W. Hensle, D. T. Chang, R. Shabsigh, C. A. Olsson, and J. P. Connor, "Laser tissue soldering in urinary tract reconstruction: First human experience," *Urology*, Vol. 46, no. 2, pp. 261–266, 1995.

86. Wider, T. M., S. K. Libutti, D. P. Greenwald, M. C. Oz, J. S. Yager, M. R. Treat, and N. E. Hugo, "Skin closure with dye-enhanced laser welding and fibrinogen," *Plas Recon Surg*, Vol. 88, no. 6, pp. 1018–1025, 1991.

87. Cooper, C. S., I. P. Schwartz, D. Suh, and A. J. Kirsch, "Optimal solder and power density for diode laser tissue soldering (LTS)," *Lasers Surg Med*, Vol. 29, pp. 53–61, 2001.

88. Suh, D. D., I. P. Schwartz, D. A. Canning, H. M. Snyder, S. A. Zderic, and A. J. Kirsch, "Comparison of dermal and epithelial approaches to laser tissue soldering for skin flap closure," *Lasers Surg Med*, Vol. 22, pp. 268–274, 1998.

89. Thomson, N. M., I. J. Simpson, D. J. Evans, and D. K. Peters, "Defibrination with ancrod in experimental chronic immune complex nephritis," *Clin Exp Immunol*, Vol. 20, pp. 527–535, 1975.

90. Naish, P. F., D. J. Evans, and D. K. Peters, "The effects of defibrination with ancrod in experimental allergic glomerular injury," *Clin Exp Immunol*, Vol. 20, pp. 303–309, 1975.

91. Kinsella, J. E., and D. M. Whitehead, "Proteins in whey: Chemical, physical, and functional properties," *Adv Food Nutr Res*, Vol. 33, pp. 343–438, 1989.

92. Kinsella, J. E., "Milk proteins: Physicochemical and functional properties," *Crit Rev Food Sci Nutr*, Vol. 21, no. 3, pp. 197–262, 1984.

93. Tabakoglu, H. O., A. Gurkan, I. Çilesiz, and M. Gulsoy, "Tissue soldering with 809-nm diode laser," *Proc 12th Natl Meet Biomed Eng*, Vol. 1, pp. 157–161, 2007.

94. Kirsch, A. J., G. M. DeVries, D. T. Chang, C. A. Olsson, J. P. Connor, and T. W. Hensle, "Hypospadias repair by laser tissue soldering: Intraoperative results and follow up in 30 children," *Urology*, Vol. 48, pp. 616–623, 1996.

95. Abergel, R. P., R. F. Lyons, R. A. White, G. Lask, L. Y. Matsuoka, R. M. Dwyer, J. Uitto, C. A. Torrance, and I. L. Springfield, "Skin closure by Nd:YAG laser welding," *J Am Acad Dermatol*, Vol. 14, pp. 810–814, 1986.

96. Gulsoy, M., Z. Dereli, H. O. Tabakoglu, and O. Bozkulak, "Closure of skin incisions by 980-nm diode laser welding," *Lasers Med Sci*, Vol. 21, pp. 5–10, 2006.

97. Dereli, Z., H. O. Tabakoglu, O. Bozkulak, A. Aksel, and M. Gulsoy, "Tissue welding with 980-nm diode laser system: preliminary study for determination of optimal parameters," in *Photonic Therapeutics and Diagnostics II: Proc. SPIE / Volume 6078 / Laser Welding and Soldering of Tissue*, pp. 607811–607818, 2006. doi: 10.1117/12.645860.

98. Niemz, M. H., *Laser Tissue Interactions*, New York: Springer, 1st edition ed., 1996.

99. McKenzie, A. L., "Physics of thermal processes in laser tissue interaction," *Phys Med Biol*, Vol. 39, no. 9, pp. 1175–1209, 1990.

100. Peavy, G. M., "Lasers and laser tissue interaction," *Vet Clin North Am Small Anim Pract*, Vol. 32, no. 3, pp. 517–534, 2002.

101. Tabakoglu, H. O., N. Topaloglu, and M. Gulsoy, "The effect of irradiance level in 980-nm diode laser skin welding," *Photomed Laser Surg*, Vol. Published Online: 21 September 2009, no. In Press. doi: 10.1089/pho.2009.2569.

102. Tabakoglu, H. O., N. Topaloglu, and M. Gulsoy, "Investigation of different modalities of laser delivery for skin welding," in *Proc 14th Natl Meet Biomed Eng*, pp. 42–49, 2009.

103. Trout, N. J., *Textbook of Small Animal Surgery*, pp. 274–290. Principles of plastic and reconstructive surgery, Philadelphia: Saunders, $3^{r}d$ ed., 2002.

104. Gobin, A. M., D. P. ONeal, D. M. Watkins, N. J. Halas, R. A. Drezek, and J. L. West, "Near infrared laser tissue welding using nanoshells as an exogenous absorber," *Lasers Surg Med*, pp. 1–7, 2005.

105. Dorsett-Martin, W. A., "Rat models of skin wound healing: A review," *Wound Rep Reg*, Vol. 12, pp. 591–599, 2004.

106. Fried, N. M., B. Choi, A. J. Welch, and J. T. Walsh, "Radiometric surface temperature measurements during dye-assisted laser skin closure: in vitro and in vivo results," *Lasers Surg Med*, Vol. 25, pp. 291–303, 1999.

107. Tabakoglu, H. O., T. Bilici, and M. Gulsoy, "Laser skin welding with 1070 nm Ytterbium Fiber Laser," in *$13^{t}h$ Conference on Laser Optics*, pp. 24–26, 2008.

108. Hitz, C. B., J. J. Ewing, and J. Hecht, "Introduction to laser technology," ch. Semiconductor lasers, pp. 182–186, New York, USA: Wiley-IEEE Press, 2001.

109. Tabakoglu, H. O., and M. Gulsoy, "In vivo comparison of near infrared lasers for skin welding," *Lasers Med Sci*, Vol. Published Online: 18 November 2009, no. In Press. doi: 10.1007/s10103-009-0739-3.

110. Katz, S., M. Izhar, and D. Mirelman, "Bacterial adherence to surgical sutures. a possible factor in suture induced infection," *Ann Surg*, Vol. 194, pp. 35–41, 1981.

111. DeCoste, S. D., W. Farinelli, T. Flotte, and R. R. Anderson, "Dye enhanced laser welding for skin closure," *Lasers Surg Med*, Vol. 12, pp. 25–32, 1992.

112. Kirsch, A. J., J. W. Duckett, H. M. Snyder, D. A. Canning, D. W. Harshaw, P. Howard, E. J. Marcarak, and S. A. Zderic, "Skin flap closure by dermal laser tissue soldering: A wound healing model for sutureless hypospadias repair," *Urology*, Vol. 50, pp. 263–272, 1997.